DOKUZ EYLÜL UNIVERSITY
GRADUATE SCHOOL OF NATURAL AND APPLIED SCIENCES

GEMMOLOGICAL AND MINERALOGICAL INVESTIGATION AND GENESIS OF SMOKY QUARTZ FROM THE AYDIN REGION

by
Hatice Gülnaz ÇİFTÇİOĞLU

October, 2014
İZMİR

GEMMOLOGICAL AND MINERALOGICAL INVESTIGATION AND GENESIS OF SMOKY QUARTZ FROM THE AYDIN REGION

A Thesis Submitted to the
Graduate School of Natural and Applied Sciences of Dokuz Eylul University
In Partial Fulfilment of the Requirements for the Degree of Master of Science in Natural Building Stones and Gemstones

by
Hatice Gülnaz ÇİFTÇİOĞLU

October, 2014
İZMİR

M. Sc. THESIS EXAMINATION RESULT FORM

We have read the thesis entitled **"GEMMOLOGICAL AND MINERALOGICAL INVESTIGATION AND GENESIS OF SMOKY QUARTZ FROM THE AYDIN REGION"** completed by **HATİCE GÜLNAZ ÇİFTÇİOĞLU** under supervision of **ASSOC. PROF. DR. MURAT HATİPOĞLU** and we certify that in our opinion it is fully adequate, in scope and in quality, as a thesis for the degree of Master of Science.

Assoc. Prof. Dr. Murat HATİPOĞLU

Supervisor

Prof. Dr. Talip GÜNGÖR

(Jury Member)

Prof. Dr. Turgay Onaraş

(Jury Member)

Prof. Dr. Ayşe OKUR
Director
Graduate School of Natural and Applied Sciences

ACKNOWLEDGMENTS

First of all, I would like to express my gratitude and special thanks to my supervisor Assoc. Prof. Dr. Murat Hatipoğlu, Dokuz Eylül University, for his guidance, patience and support, as well as his understanding. I appreciate his time and effort in helping to write this thesis and greatly value his assistance.

Second, I would like to give my sincere thanks to Prof.Dr. Cahit Helvacı (Dokuz Eylül University), Prof.Dr. Turgay Karalı (Ege University) and Prof.Dr. Nurdoğan Can (Celal Bayar University) for their help.

And, of course, I would like to give my special loves to my parents, for their support and encouragement in everything I do. Thankyou!

Hatice Gülnaz ÇİFTÇİOĞLU

GEMMOLOGICAL AND MINERALOGICAL INVESTIGATION AND GENESIS OF SMOKY QUARTZ FROM THE AYDIN REGION

ABSTRACT

Quartz crystals with some impurity ions can absorb energy from ionizing radiation, e.g. gamma rays. This absorption of energy can influence its optical and electromechanical performance, thermal characterisation, as well as its color. Natural gem-quality dark brown (morion type) smoky quartz specimens from the Aydin region were investigated using the chemical analyses (XRF, ICP-AES), microscopical observations (PM), X-ray diffraction (XRD), spectroscopic evaluationsinfrared vibration (IR), simultaneous differential thermal and thermo gravimetric analysis (DTA/TGA), radioluminescence (RL), and Thermoluminescence (TL), to reveal and discuss their physic-chemical and geochemical formation conditions.

One of the most important gem material of Turkey, smoky quartz crystals, werestudied for color saturation from the mineralogicalgenetic view point. Color formation in the smoky quartzes is due to the color centres which are produced in the result of exposing to mainly gamma irradiation of some substituted impurity elements in SiO4 tetrahedral in the quartz lattice. When the optical absorption graphics (OA) comprising the ultraviolet, visible, and near-infrared regions and the impurity elements (ICP and AES) are evaluated collectively, four main absorption bands are related to producing the color centres Accordingly, in the morion type smoky quartzes, the absorption peaks at 375 nm, 450 and 490 nm, 620 nm and 730 nm is due to Al3plus, Ti4plus, Fe2plus, Mn2plus ions respectively.

Radioluminescence (RL) graphics can be used as an effective method showing the color centres exposed to irradiation in the mineral lattice. The RL graphic of natural smoky quartz crystals displays that the most affected impurity elements after exposing to additional gamma irradiation in the crystalline structure are Fe and Al elements with 3plus valance value substituted for Si4plus in the smoky quartz silica

lattice. Accordingly, Fe3plus ion representing the RL band at 600 nm, Al3plus ion representing the RL band at 720 nm, Mn2plus ion representing the RL band at 385 and 410 nm, and Ti4plus ion representing the RL band 495and 510 nm.

The IR transmission stretching curve of smoky quartz samples were recorded on standard axes in the measured range (4.000 and 400 cm minus1). Accordingly, the some collective and crosswise vibration bands of the smoky quartz samples were compared with peaks of the colorless quartz sample.

Thermal behaviors of the smoky quartz samples were investigated using the thermograms of the simultaneous differential thermal and thermogravimetric analyses (DTA/TGA) from room temperature up to 1400 degrees Celcius to observe the changing ratios in their water contents and enthalpy during dehydration.

Keywords: Natural morion type smoky quartz, gemmology, gemstone, Çine and Karacasu and Koçarlı regions (Aydın), irradiation, color saturation, spectroscopy.

AYDIN BÖLGESİ DUMANLI KUVARSININ GEMOLOJİK VE MİNERALOJİK İNCELEMESİ VE OLUŞUM KÖKENİ

ÖZ

Bir takım kimyasal iz elementler içeren kuvars kristalleri, gama ışınları gibi iyonlaştırıcı radyasyondan enerji emebilir. Bu enerji emilimi, kuvarsın görsel ve elektromanyetik performansını, termal özelliğini ve rengini etkileyebilir. Fiziksel-kimyasal ve jeokimyasal oluşum şartlarını ortaya çıkarmak ve üzerinde tartışmak için, Aydın yöresinden alınan doğal, süstaşı kalitesindeki, kahverenkli (morion tipi) dumanlı kuvars örnekleri, kimyasal analizler (XRF, ICP ve AES), mikroskopik gözlemler (PM), X ışını kırınımı (XRD), spektroskopik değerlendirmeler kızılötesi titreşimler (IR), eşzamanlı diferansiyel termal ve termo ağırlık analizi (DTA/TGA), radyolüminesans (RL) ve termolüminesans (TL) kullanılarak incelenmiştir.

Türkiye'nin en önemli süstaşlarından biri olan dumanlı kuvars kristalleri, minerolojik köken açısından ideal renk doygunluğu için bu çalışma süresince incelenmişlerdir. Dumanlı kuvarslarda renk oluşumu, kuvars kafesindeki SiO4 tetrahedralindeki bir takım safsızlık elementlerinin, özellikle gama ışımasına maruz kalması sonucu renk merkezleri oluşturmasıylameydana gelmektedir. Ultraviyole, görünür ve yakın infrared bölgelerini kapsayan optik absorbsiyon grafikleri (OA) safsızlık elementlerini (ICP ve AES) içeren kimyasal analizler birlikte değerlendirildiğinde, dört ana soğurum bandının, renk merkezlerini oluşturmasıyla bağlantılı olduğu görülmektedir. Bu nedenle morion tipi dumanlı kuvarslarda, 375 nm, 450 ile 490 nm, 620 nm ve730 nm, deki soğurma pikleri sırasıyla Al3artı, Ti4artı, Fe2artı, Mn2artı iyonlarına bağlı olarak oluşmuştur.

Radyolüminesans grafikleri (RL), mineral kafesindeki radyasyona maruz kalmış renk merkezlerinin varlığını ortaya çıkartan etkili bir yöntem olarak kullanılabilir. Doğal dumanlı kuvars kristallerinin RL grafiği göstermektedir ki, kristal yapıda ilave gama ışıması sonucu en fazla etkilenen safsızlık elementleri artı3 valans değerine sahip Fe ve Al elementleridir. Bunlar dumanlı kuvarsın kafesindeki Si4artı ile yer

değiştiren elementlerdir. Bu nedenle, Fe3artı iyonu 600 nm deki RL bandını, Al3artı iyonu 720 nm deki RL bandını, Mn2artı iyonu 385 ile 410 nm deki RL bandını ve Ti4artı iyonu 495 ile 510 nm de RL bandını temsil eder.

Dumanlı kuvars örneklerinin IR geçirim gerilme eğrisi, (4.000 ile 400 cmeksi1)ölçüm aralığındaki standart eksen üzerine kaydedilmiştir.Ortak ve çapraz titreşim bantları renksiz kuvars örneklerinin pikleriyle kıyaslanmıştır.

Dumanlı kuvars örneklerinin termal davranışları, 1400 santigrad dereceye kadar oda sıcaklığından alınan eş zamanlı diferansiyel termal ve termogravimetrik analizlerinin (DTA/TGA) termogramları kullanılarak incelenmiştir. Amaç, su hacimlerindeki değişen oranları, su hakim oranlarını ve dehidrasyon esnasındaki ısı içeriğini gözlemektir.

Anahtar kelimeler: Doğal morion tipi dumanlı kuvars, gemoloji, süstaşı, Çine ve Karacasu ve Koçarlı bölgeleri (Aydın), radyasyon ışıması, renk doygunlaşması, spektroskopi.

CONTENTS

Page

THESIS EXAMINATION RESULT FORM ii
ACKNOWLEDGEMENTS iii
ABSTRACT iv
ÖZ vi
LIST OF FIGURES x
LIST OF TABLES xii

CHAPTER ONE – INTRODUCTION 1

1.1 Description of Smoky Quartz 1
1.2 Localities in Turkey 4
1.3 Crystalline Quartz Structure 5
1.4 The Usage of Irradiation in the Quartzes for Color Saturation 6
1.5 Aims and Scope 7

CHAPTER TWO – MATERIALS AND METHODS 8

CHAPTER THREE – RESULTS AND DISCUSSION 12

3.1 Provenance and Geological Setting 12
3.2 Geo-Chemistry (XRF and ICP-AES) 13
3.3 Mineralogy (Microscopical and Spectroscopical) 14
3.3.1 Polarizing Microscopy (PM) 14
3.3.2X-Ray Diffraction Spectroscopy (XRD) 16
3.3.3 Optical Absorption (OA) 20
3.3.4Infrared Spectroscopy (IR) 23
3.3.5 Simultaneous Differential Thermal and Thermo Gravimetric Analysis (DTA/TGA) 31
3.3.6 Thermoluminesence Spectroscopy (TL) 34
3.3.7 RadioluminescenceSpectroscopy (RL) 36

3.4 Gemmology 37

CHAPTER FOUR – CONCLUSIONS..... 40

REFERENCES..... 42

LIST OF FIGURES

Page

Figure 1.1 Main investigation material of this study; natural dark rough smoky quartzes..... 4

Figure 1.2 Loose and matrix specimens morion type smoky rough quartz crystals .. 5

Figure 1.3 Framework of SiO_4 silicon-oxygen tetrahedra with each oxygen being shared between two tetrahedral 6

Figure 2.1 Olympus BX41 binocular polarizing microscope with a high-intensity 6V, 30W halogen light source combined with U-CPA and U-OPA optical systems in Department of Geological Engineering of Dokuz Eylul University 9

Figure 2.2 The device comprised of a DTG-60H Simultaneous DTA-TG Apparatus and a Data Collector TA-60 WS Thermal Analyzer in the Material Investigation Laboratory of Faculty of Engineering in Dokuz Eylul University 10

Figure 2.3 Shimadzu IR-470 transmission infrared spectrophotometer in the Material Investigation Laboratory of Institute of Nuclear Sciences in Ege University ……11

Figure 3.1 Landscape viewing obtained from the satellite of quartz veins in the Bağcılar and Esentepe smoky quartz minefields in the Koçarlı (Aydın) region..... 12

Figure 3.2 The XRD graphic of smoky quartz sample of the Aydın region, showing joint silica phases Q-M-*O*S, Q-M-L, Q-M and single silica phases Q and M 17

Figure 3.3 Optical absorption (OA) graphics natural smoky quartz specimen of the Aydın region..... 21

Figure 3.4 Optical absorption spectra (OA) of natural smoky quartz of Aydın region, and of after exposing to artificial gamma, neutron and beta irradiations 22

Figure 3.5 The IR transmission spectrum of natural morion type smoky quartz..... 23

Figure 3.6 The IR transmission spectrum of natural dark (morion type), light smoky quartzes and colorless quartz for comparison and contrast to each other 24
Figure 3.7 Ideal infrared (IR) graphic in the range 26
Figure 3.8 Simultaneous DTA/TGA thermogram of natural morion type smoky quartz. 33
Figure 3.9 Thermoluminescence glow curves of natural morion type smoky quartz. 35
Figure 3.10 Radioluminescence (RL) spectra of natural and various irradiated smoky quartzes from the Aydın region 36
Figure 3.11 Facet cut and polished gemstones with various lapidary forms of light and morion type smoky quartz from the Aydın region. 37
Figure 3.12 Cabochon cut and polished gemstones with various lapidary forms of light and morion type smoky quartz from the Aydın region 38
Figure 3.13 Smoky quartz mine field in the Aydın-Koçarlı-Bağcılar and Esentepe regions 39

LIST OF TABLES

Page

Table 1.1 An overview of the "modern" classification scheme, and lists all varieties.2

Table 1.2 The most important properties are listed for comparison. One notable difference is that the numerical values for refractive index, specific weight, and hardness of macrocrystalline quartz are *exact*, while the values given for cryptocrystalline quartz are approximations 3

Table 3.1 Chemical bulk and trace element analyses of the natural smoky quartz sample from Turkey..... 13

Table 3.2 The XRD numerical data of smoky quartz sample of the Aydın region.... 18

Table 3.3 The infrared (IR) vibration peaks in the ranging between 400 and 1100 cm^{-1} of natural morion type smoky quartz sample. 28

Table 3.4 The infrared (IR) vibration peaks in the ranging between 1100 and 3000 cm^{-1} of natural morion type smoky quartz sample 30

Table 3.5 The infrared (IR) vibration peaks in the ranging between 3000 and 4000 cm^{-1} of natural morion type smoky quartz sample. 31

Table 3.6 Thermogram data of weight change (TGA) of natural morion type smoky quartz 33

Table 3.7 Thermogram data of endothermic and exothermic cumulative temperature change (DTA) depending upon differentiation of smoky quartz 33

CHAPTER ONE
INTRODUCTION

1.1 Description of Smoky Quartz

"Quartz" is a term that includes both well-crystallized and compact forms of silica. For the most time, the different quartz varieties have been considered as species of their own and have not been systematically grouped together before the 19th century. Their common chemical nature was discovered by the Swedish chemist Bergmann at the end of the 18th century, and for some time silica was considered a chemical element. In 1823, his fellow countryman J.J. Berzelius decomposed quartz and discovered it is the chemical compound of oxygen and a new element, silicon. After it was realized that all those varieties are chemically the same substance, silicon dioxide (SiO_2), they were divided into groups (Back & Mandarino, 2008; Florke et al., 1991; Fritsch et al., 2002; Graetsch, 1994; Heaney, 1994; Heaney et al., 1994; Heaney & Banfield, 1995; Iller, 1979; Smith, 1998).

Today, most authors use a different scheme for classification. The crystalline forms are commonly calledmacrocrystalline quartz, while the dense and compact forms are either called cryptocrystalline or microcrystalline quartz (Table 1.1). When people talk about "quartz", they often mean macrocrystalline quartz, whereas cryptocrystalline varieties are often subsumed under the term chalcedony.

Table 1.1 An overview of the "modern" classification scheme, and lists all varieties. The distinction between "fibrous" and "grainy" varieties is based on the visual appearance of thin sections in a polarizing microscope.

Macrocrystalline Quartz or simply **"Quartz"**	**Crypto- or Microcrystalline Quartz** or simply **"Chalcedony"**
	"Fibrous" Varieties:
1.Rock Crystal	1.Kalsedon
2.Smoky Quartz (Morion)	2.Agate
3.Amethyst	3.Carnelian
4.Ametrine	4.Chrysoprase
5.Aventurine	5.Plasma
6.Blue Quartz	6.Onyx
7.Citrine	7.Sard
8.Milky Quartz	8.Sard Oniks
9.Pink Quartz	**"Grainy" Varieties:**
10.Prase	1.Chert
11.Prasiolite	2.Flint
12.Rose Quartz	3.Jasper
13.Tiger's, Hawk's, and Cat's Eye	4.Heliotrope
	5.Plasma

It has been found that the causes for the differences in structure, physical properties, and visual appearance lie primarily in the environmental conditions during the formation of the minerals:

Macro- and cryptocrystalline forms of quartz differ in the way they grow.

*Macrocrystalline quartz grows by adding molecules to the crystal's surface, layer by layer.

*Cryptocrystalline quartz forms from a colloidal watery solution of silica.

It should be noted that this is still an oversimplification and that there are cases that do not fit well in that classification scheme, in particular the formation of certain rocks made of chert and certain rocks made of a silica sinter. The first sometimes forms from opaline sediments or glassy volcanic ashes, the latter is observed in low and medium temperature, low-pressure veins, and in geysers, often together with opaline sinter. Both assume a cryptocrystalline structure (similar in look to flint and jasper) but do not form from gel-like colloidal precursors. The formation of the "grainy varieties" like jasper and flint and their respective sub-varieties also seems to deviate in some ways from that of "ordinary" fibrous chalcedony. The specific

properties of macro- and cryptocrystalline quartz are simply a consequence of the way they form (Table 1.2)

The reason is that cryptocrystalline quartz varieties mostly consist of microscopically small intergrown quartz crystal grains, so they lack the structural homogeneity of crystals. Their final structure varies with the environmental conditions and also depends on the amount of impurities that have been embedded during formation. Strictly spoken, cryptocrystalline varieties don't count as minerals, they are so-called textural varieties of quartz, and more similar to rocks (like marble or quartzite). They contain relatively large amounts of other silica modifications, water and other non-silica minerals. The mineralogy of macrocrystalline quartz, on the other hand, is fairly straightforward, and if it wasn't for its abundance and its important role in many different geological environments, there would not be so much to say about it. One notable mineralogical property of quartz is that clear crystals, even those of colored varieties, are remarkably pure.

Table 1.2 The most important properties are listed for comparison. One notable difference is that the numerical values for refractive index, specific weight, and hardness of macrocrystalline quartz are *exact*, while the values given for cryptocrystalline quartz are approximations.

	Macrocrystalline	**Cryptocrystalline**
Color	Any	Any
Diapheny	transparent-translucent	translucent-opaque
Luster	Vitreous	waxy – dull
Luster on Fractures	vitreous – fatty	Dull
Streak	White	white, slightly colored
Refractive Index	1.544-1.553	1.53-1.54
Specific Weight	2.65 g/cm^3	2.4-2.7 g/cm^3
Hardness	7	6.5-7
Water Content	<< 0.1%	0.1-4%
Non-Silica Impurities	0.01% - 0.5%	1% - 2%

Smoky quartz (light and dark (morion type) colored),(Figure 1.1), which is the main investigation material of this study, is a crystalline quartz species, and has been known the most commonly used materials for the making of jewelry and hardstone carving since the antiquity.The crystals frequently contain inclusions of gas (carbon dioxide), liquid (often both water and liquid carbon dioxide), or solids (rutile). Smoky quartz from Mount Cairngorm, Scotland,is known as cairngorm and is a favorite ornamental stone in Scotland.

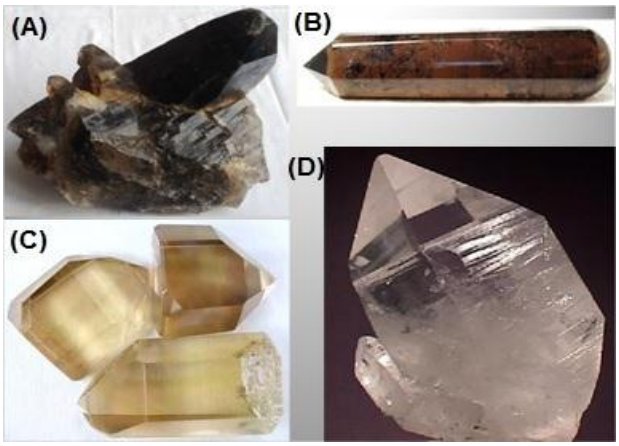

Figure 1.1 Main investigation material of this study;natural dark (morion type) [(A) and (B)]and light [(C) and (D)] rough smoky quartzes.

1.2 Localities in Turkey

Gem quality morion type smoky quartz crystals (dark smoky colored)are found economic reserves in natural deposits of Turkey, especially the Koçarlı-Karacasu-Çine regions in Aydın(Figure 1.2).Quartz veins in gneiss and schist are exposed at the surface.



Figure 1.2 Loose and matrix specimens morion type smoky rough quartz crystals.The crystals range from finger size to arm size (**a**) and (**c**). Irregular facet cut and polished smoky quartz gems showing various shades of brown (**b**), famous localities in Turkey (**d**). Quartz veins in gneiss and schist are exposed at the surface where they can be exploited by villagers (**e**). Stock of rough black quartz crystals (morion) extracted by a professional collector Musa Ceylan from Esentepe Yayla village (modified from Hatipoğlu et al., 2010a).

1.3 Crystalline Quartz Structure

The mineral quartz with an overall formula $SiO_2$is made up of a continuous framework of SiO_4 silicon-oxygen tetrahedra with each oxygen being shared between two tetrahedra (Figure 1.3). Smoky quartz includes Al, Fe, Ti and Mn impurity elements as over 100 ppm in richness. In addition, Na, K, Ca and Mg are present in sufficient quantities more than 100 ppm as the elements adding their

valance in the silica lattice of both species.Detailed reviews of Al-centers in quartz have been provided by Lehmann and Moore (1966), Weil (1984), and Halliburton (1989).

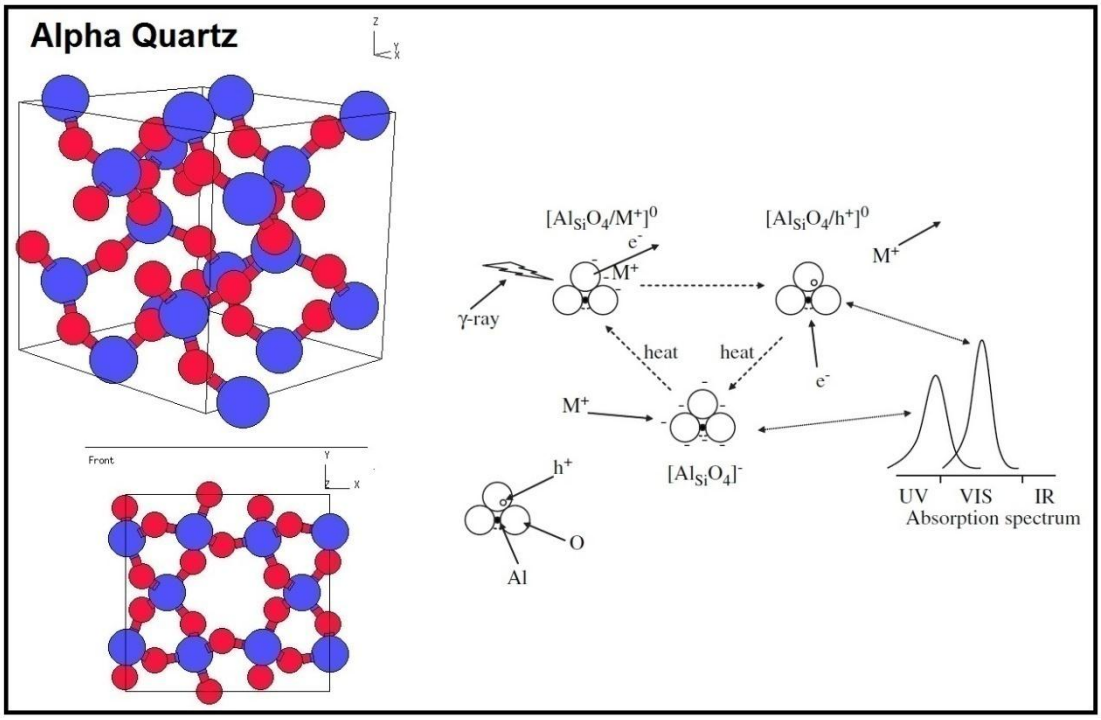

Figure 1.3 Framework of SiO_4 silicon-oxygen tetrahedra with each oxygen being shared between two tetrahedra. Alpha quartz with aluminium as impurity absorbs energy from ionizing radiation and modifies its color (After Halliburton, 1989).

The most important mineralogical characterization for the mineral quartz is piezoelectricity. The first application of piezoelectric effect ofquartz was made by Langevin in 1917, after thediscovery of piezoelectric effect by Curie brothersin 1880 (Iler, 1979).

1.4 The Usage of Irradiation in the Quartzes for Color Saturation

It is improved with experimental via synthetic productions of smoky quartz crystals that light and dark smoky colored formations are due to the color centres which are produced in the result of exposing to mainly gamma irradiation of some substituted impurity elements (mainly iron and aluminium) in SiO_4 tetrahedral in the

quartz lattice. Several studies have been reported in which artificial irradiationmethods have been used for color saturation on smoky quartz crystals (Bahadur, 1989; Balitsky et al., 2002; Dudeshenko et al., 2004; Halliburton, 1989).

1.5 Aims and Scope

In nature, the geochemical formation agents of the natural macrocrystalline structured silica mineral species arise as the essential question to be explored. In this study, the main interest was given to investigate mineralogical features, such as textural, chemical, micro-structural and spectral characteristics of natural gem-quality morion type smoky quartz specimens.

Smoky quartz crystals are desired and demanded in relatively high values in worldwide gem market, when they have the saturated colorations, such as dark brown or blackish, instead of that of pale smoky colorations. For this reason, many deposits including large quantities of industrial low quality gem material have been abandoned in both Turkey and the World. Smoky quartzes may become greenish, yellowish, darkbrownish or colorless after heat-treatment. Natural, colorless quartz is routinely colored by irradiation with gamma rays and heat-treatment for jewellery production.

At the present day, the enhancement endeavours to find alternative color saturation and color changing are still continued to become economic these out of use industrial materials, because the heating stimulus treated to transparent morion type smoky quartz is very risk as a destructive color enhancement method.

Ultimately, after pale low quality smoky quartz crystals are exposed to gamma, neutron and beta irradiations, it is seen that the effective color saturation of dark colored smoky quartz is enhanced only by artificial gamma irradiation stimulus. On the other hand, gamma irradiation for turning progress to yellow coloration to produce citrine rarely found naturally cannot be an alternative treatment method instead of traditional artificial heating stimulus.

CHAPTER TWO
MATERIALS AND METHODS

Samples of morion type smoky quartz were especially chosen from the Koçarlı (Aydın) region, because of the both excellent saturated dark brown and blackish) and dull or pale colors.

For the determining the impurity elements, the XRF for major oxides, ICP-AES for trace elements and WST-SIM for loss of igneous techniques by the accredited ALS Chemex Laboratory-Canada was performed. Certificate numbers are IZ11005163 and IZ09053895.

For the polarizing microscope observations, slices of 10 x 10 x 1 mm^3were cut from the representative samples with the square faces perpendicular and parallel to the "c" crystal axis. Both sides of the slices with various thicknesses were mechanically polished with four different diamond pastes from 200 to 3000-mesh. The samples were investigated by using a XY-P1 type transmitted polarization microscope that was equipped with gyps λboard, mica λ/4 board, quartz wedge and mechanical stages.Polarizing microscope images of thin sections of the sampleswere obtained by using an Olympus BX41 binocular polarizing microscope with a high-intensity 6V, 30W halogen light source combined with U-CPA and U-OPA optical systems (Figure 2.1). For the digital images, the microscopic magnification (MM) was 4x (resulting from 0.4x objective and 10x ocular) and 10x (1x objective and 10x ocular) under crossed nicols (+N) (active polarizer and analyzer).

Optical absorption spectra (OA) of the both natural and artificial irradiated samples were taken using Varian DMS 90 UV/VIS and Sosco Model 7800 UV/VIS Spectrophotometers in the range of 200-800 nm.

The silica building phases of the samples were taken by the same XRD device using a Philips X'Pert Pro instrument. The instrument used 1.5405600 Å for K-

Alpha1 and 1.5443900 Å for K-Alpha2. The initial and final wavelengths for the samples were between 5.00 and 80.00 $^{o}2\theta$.



Figure 2.1 Olympus BX41 binocular polarizing microscope with a high-intensity 6V, 30W halogen light source combined with U-CPA and U-OPA optical systems in Department of Geological Engineering of Dokuz Eylul University.

The thermogram curves of the samples were analyzed using the Shimadzu device (Figure 2.2), which does a simultaneous DTA-TGA analysis to determine changes in weight and heat energy against temperature in the samples and plots them graphically. This instrument or testing technique may be called a Simultaneous Thermal Analysis (STA). The resulting DTA and TGA curves were simultaneously plotted on a dual Y-axis graphic, so the DTA's fingerprint and the TGA's weight loss/gain characteristics were directly compared as the investigated silica varieties were heated. The device comprised of a DTG-60H Simultaneous DTA-TG Apparatus and a Data Collector TA-60 WS Thermal Analyzer. In the graphics, the change of TGA and DTA are "mg" and "Microvolt" respectively. In the process of analyzing samples, nitrogen (N_2) was used intensively in the device in addition to the

gas existing in the atmosphere. All samples were in solid form, and their weights were in approximately 50 mg (± 6 mg).



Figure 2.2 The device comprised of a DTG-60H Simultaneous DTA-TG Apparatus and a Data Collector TA-60 WS Thermal Analyzer in the Material Investigation Laboratory of Faculty of Engineering in Dokuz Eylul University.

Dull or pale colored smoky quartz samples were irradiated with gamma, neutron and beta beams. The temperature in the irradiation room was in the range of 15°C to 35°C. For gamma (γ) irradiation, a Gammacell-220 dry gamma irradiator device was used. Its radioactive material is Co^{60}. Its radiation energy is 12.400 Ci and I=0.08 Mrad. The samples were irradiated for 24 and 43 hours. For neutron irradiation, a Siemens device was used. The samples were irradiated by 3 MeV-neutrons with two different neutron fluxes. After 2 hours 20 minutes, 15.15×10^{7} n/cm^{2} were counted in the monitor for the first group. After 2 hours 50 minutes, 20.42×10^{7} n/cm^{2} were counted in the monitor for the second group. For beta (β) irradiation, Siemens Betatron-500A device was used and the samples were irradiated for 10 minutes in a 7 MeV-electron each at 800 pulses-2.000 rad and 1600 pulses-4.000 rad.

For radioluminescence (RL) measurements of natural and irradiated samples, a Yobin Yuan spectrophotometer coupled with a CCD detector is used. X-ray irradiation was supplied via a tungsten X-ray tube (Machlett OEG-50A) with a

current setting of 15 mA and a voltage of 30 kV, delivering a dose rate of 10 Gy min^{-1} to the samples. Signals were recorded over the wavelength range of 200-800 nm.

The vibration stretching bands and peaks in near infrared region of the samples were recorded in the 400 to 4000 cm^{-1} range with a Shimadzu IR-470 transmission infrared spectrophotometer (Figure 2.3) using the KBr (potassium bromide) powder pellet technique under standard laboratory conditions. The resolution of transmission spectra of the samples are displayed as percentages from 0 to 100. This resolution is acceptable as high. In the process of analyzing samples, the carbon dioxide (CO_2) was used intensively in the device in addition to the gas existing in the atmosphere.



Figure 2.3 Shimadzu IR-470 transmission infrared spectrophotometer in the Material Investigation Laboratory of Institute of Nuclear Sciences in Ege University.

CHAPTER THREE
RESULTS AND DISCUSSION

3.1 Provenance and Geological Setting

Morion type smoky quartz crystals in the Aydın region are filled into the post-metamorphic tension fractures with E-W direction formed during the Late Oligocene Period (about 23.8-28 Myr)**,** cutting the schist and gneiss metamorphic basement rocks (Collins & Robertson, 2003).

When it is considered the geological formation conditions of smoky quartz crystals with macrocrystalline structure and crystalline shape, they are generated in the silica-bearing host rocks of the Tertiary Period in the Aydın region of Turkey. The crystals are occurred at the ambient silica-bearing conditions from the hydrothermal solutions including silicic acid (H_4SiO_4) in the suitable pores, vesicles, veins, joints and cracks of their surrounding host rocks (Figure 3.1).



Figure 3.1 Landscape viewing obtained from the satellite of quartz veins in the Bağcılar and Esentepesmoky quartz minefields in the Koçarlı (Aydın) region. The veins and lenses of smoky quartz crystals occur in host rocks such as gneisses and schists. They were formed by hydrothermal solutions rich in silica that penetrated and mineralized fractures in these rocks near the center of the Menderes Massif basin. Such hydrothermal mineralization has occurred repeatedly over a long period, ending only in the recent geological past.

3.2 Geo-Chemistry (XRF, ICP-AES)

Table 3.1 shows chemical main silica bulk analyses of the investigated natural smoky quartzsamples.

It is seen that Al_2O_3 is the relatively highest. Therefore, itcan be assigned the rich AlO_4 sites in the smoky quartz samples. In addition, Na_2O is very important an electrolyte for the precipitation from the silicic acid (H_4SO_4) rich hydrothermal solutions of all the kind of silica in nature (Krauskopf, 1982; Landmesser, 1995).

Table 3.1 Chemical bulk and trace element analyses of the natural smoky quartz sample from Turkey.

Oxides %	Instrument	Element	Instrument	Instrument	Element
		Smoky Quartz			**Smoky Quartz**
SiO_2	XRF	98.45			
Al_2O_3	XRF	0.12	**Al**	ICP-AES	**0.09 %**
Fe_2O_3	XRF	1.17	**Fe**	ICP-AES	**0.84 %**
TiO_2	XRF	0.02	**Ti**	ICP-AES	**<0.01 %**
MnO	XRF	0.08	**Mn**	ICP-AES	**554 ppm**
Cr_2O_3	XRF	<0.01	Cr	ICP-AES	5 ppm
Na_2O	XRF	0.02	Na	ICP-AES	0.01 %
K_2O	XRF	0.03	K	ICP-AES	0.02 %
CaO	XRF	0.06	Ca	ICP-AES	0.04 %
MgO	XRF	0.08	Mg	ICP-AES	0.01 %
SrO	XRF	0.01	Sr	ICP-AES	4 ppm
BaO	XRF	<0.01	Ba	ICP-AES	30 ppm
P_2O_5	XRF	0.014	P	ICP-AES	30 ppm
LOI	XRF	-0.08	Ag	ICP-AES	<0.5 ppm
Total	XRF	**99.98**	As	ICP-AES	6 ppm
			Be	ICP-AES	<0.5 ppm
			Bi	ICP-AES	<0.2 ppm
			Cd	ICP-AES	<0.5 ppm
			Co	ICP-AES	1 ppm
			Cu	ICP-AES	5 ppm
			Ga	ICP-AES	<10 ppm
			La	ICP-AES	<10 ppm
			Mo	ICP-AES	1 ppm
			Ni	ICP-AES	4 ppm
			Pb	ICP-AES	3 ppm
			S	ICP-AES	0.02 %
			Sb	ICP-AES	<5 ppm
			Sc	ICP-AES	<1 ppm
			Th	ICP-AES	<20 ppm
			Ta	ICP-AES	<10 ppm
			U	ICP-AES	<10 ppm
			V	ICP-AES	3 ppm
			W	ICP-AES	<10 ppm
			Zn	ICP-AES	8 ppm

It is synthetically proved that certain impurity elements produce the color centers (Balitsky et al., 2002; Nunes & Lameiras, 2005). However, the kinds and oxidization

states of the impurity elements have already conflicted. Al and Fe elements are the most accepted and investigated impurity elements (Cohen, 1956; Cohen & Hassan, 1974; Cortezao et al., 2003); Koumvakalis, 1980; Lehman & Moore, 1966; Nassau, 1978). It is well-known that the producing of the color centers of these impurity elements without being irradiation is impossible. Thus, quartz crystal species with some impurity elements absorbs energy from ionizing radiation and modifies its color because of producing the color centres. The most effective irradiation is gamma beams for smoky quartz species (Dudeshenko et al., 2004; Halliburton et al., 1981; Nunes & Lameiras, 2005).

3.3 Mineralogy (Microscopical and Spectroscopical)

3.3.1 Polarizing Microscopy (PM)

Even if the numerical peak values of the spectroscopic devices (such as X-ray diffraction and micro-Raman) give more certain results on the detection and separation of all the kind of silica building phases, polarizing microscope can also help in detection of the silica building phases in all kind of silica species. However, the polarizing microscope images are in some casesinsufficient for both identify and quantify of crystallinity degree of the silica samples (Pretola, 2001).The some kinds of silica building phases are seen as special shapes of textures (i.e. fine or granular massive, tabular, and fibrous etc) under polarizing microscope.

Prior to spectroscopic investigations in this study, thin sections of the smoky quartz were prepared, and after then, they were microscopically examined under the polarizing microscope whether or not they contain both length-fast and length-slow silica building phases using the gypsum accessory plate for determination of their positive or negative elongation (Flörke et al., 1976 & 1991; Graetsch et al., 1987).

So, two terms bring into clear as alpha quartz and quartzine. The term "quartzine" was used in general as collectively name including moganite, orthorhombic silica and lutecite (Florke et al., 1991; Miehe & Graetsch, 1992; Murashov & Svishchev,

1998; Smith, 1998). Although quartzine only includes lutecite in the past, detailed x-ray investigations of various natural microcrystalline forms of silica in the near past, previously believed to be ordinary ‘quartz, revealed the subtle differences in silica structures. ‘Lutecite’ has known for a long time and was the name given to the samples with c at an angle of approximately 30° to the long axis of the fibers. It has monoclinic form (Florke et al., 1991). ‘Moganite’ was the name firstly given in 1976 by Florke et al. It has also monoclinic form. Latter, the silica phase called length-slow (Florke et al., 1984; Miehe et al., 1984). Recent X-ray studies have shown that length-slow varieties of microcrystalline quartz, previously labelled "lutecite," actually contain high concentrations of "moganite" (Heaney & Post, 1992). So, moganite occurs in virtually all types of fine-grained silica varieties as well petrified wood. ‘Orthorhombic Silica’ was revealed in nearer past by computer simulations as another distinct quartz-like of silica and mostly called *o*-silica (Murashov & Svishchev, 1998).

This observation is important because length-slow quartzes (moganite with monoclinic crystal system, *o*-silica with orthorhombic crystal system and lutecite with monoclinic crystal system) have positive elongation whereas length-fast quartzes (quartz with trigonal-or hexagonal crystal system and quartz-rich chalcedony with trigonal-or hexagonal crystal system as well trydimite of opal-CT and cristobalite of opal-C with trigonal-or hexagonal crystal system) have negative elongation. In an elongated crystal, one determines the optic sign by rotating the elongated grain 45 deg. from its extinction orientation and inserting the quartz plate. If the interference colors rise (turn blue in the case of quartz), the mineral has positive elongation. If the interference colors fall (turn yellow), it is negative (Heaney & Post, 1992; Pretola, 2001).

As a result of these observations,it is seen that the investigated smoky quartz samples, as an crystalline silica mineral specie, have not only homogenous plate-shaped massy silica building materials, but also, mainly heterogeneous coarse particles and partially fibrous bundle-like silica building materials. These silica materials mostly show negative elongation signifying alpha quartz and/or chalcedony

(length-fast quartz), and partially show positive elongation signifying quartzine (length-slow quartz). However, it can be said that smoky quartzes include crystalline texture.

3.3.2 X-Ray Diffraction Spectroscopy (XRD)

Nomenclature of silica varieties afore-mentioned are mainly based on their silica building phases, such as (1) quartz silica building phases (e.g. α- and β-quartzes, trydimite, low-cristobalite), (2) chalcedonic quartz silica building phases (e.g. quartz-rich chalcedony, moganite, orthorhombic silica, lutecite), and (3) opaline quartz silica building phases (e.g. opal-CT, opal-C, and opal-A) (Elzea et al., 1994; Florke et al., 1984; Fritsch et al., 2006; Gislason et al., 1997; Gotze et al., 1998; Heaney & Post, 1992; Heaney et al., 1994, 1995 & 2007; Jones & Segnit, 1971; Miehe et al., 1984; Miehe & Graetsch, 1992; Murashov & Svishchev, 1998; Nagase & Akizuki, 1997; Rodgers & Cressey, 2001; Sanders, 1970; Smith, 1992).

The X-ray diffraction patterns (XRD) of the investigated smoky quartz samples were taken to obtain their primary d-spacing ($D(I_0)$) and relative peak intensity (%) data. The representative graphic and numerical data are given in Figure 3.2 and Table 3.2

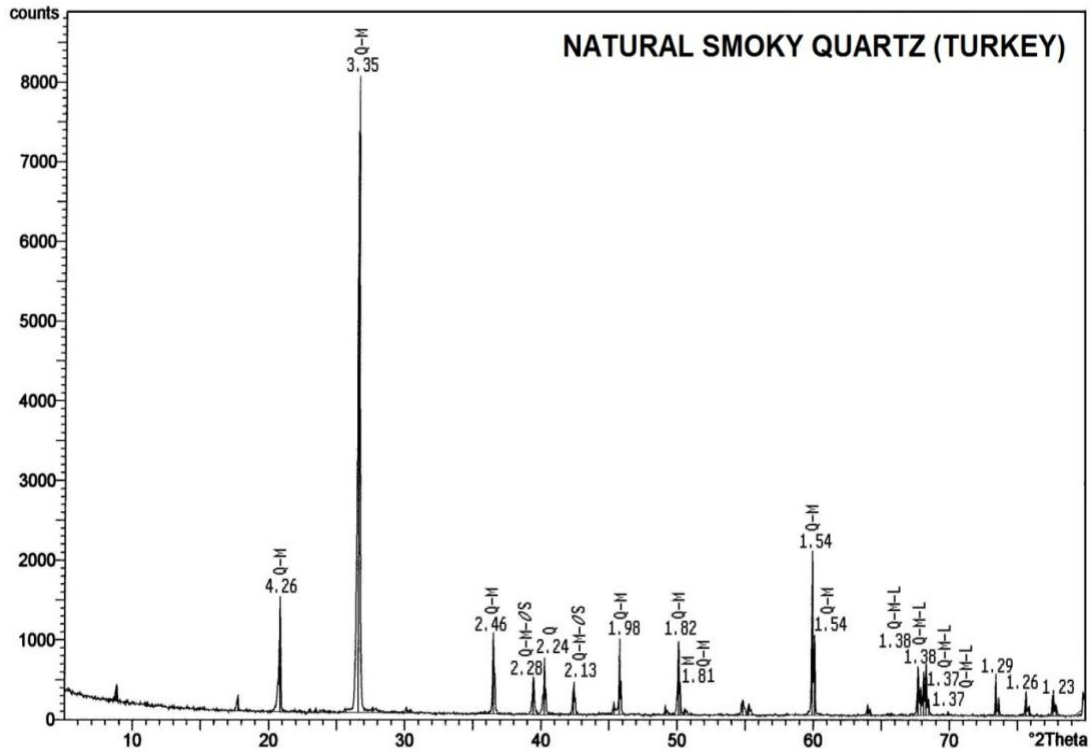

Figure 3.2 The XRD graphic of smoky quartz sample of the Aydın region, showing joint silica phases Q-M-*O*S (quartz, moganite and *o*-silica combination), Q-M-L (quartz, moganite and lutecite combination), Q-M (quartz and moganite combination), and single silica phases Q (quartz) and M (moganite). Some peaks were not matched.

Table 3.2 The XRD numerical data of smoky quartz sample of the Aydın region.

X'Pert Software
(searched) peak list: DEU-Dark smk Q

Original scan: DEU-Dark smk Q
Description of scan:

Used wavelength:	K-Alpha1
K-Alpha1 wavelength (Å):	1.5405600
K-Alpha2 wavelength (Å):	1.5443900
K-Alpha2/K-Alpha1 intensity ratio :	0.5000
K-Alpha wavelength (Å):	1.5405600
K-Beta wavelength (Å):	1.3922200
Peak search parameter set:	**As Measured Intensities**
Set created:	06/05/2005 13:24
Peak positions defined by:	Minimum of 2nd derivative
Minimum peak tip width (°2Theta):	0.00
Minimum peak tip width (°2Theta):	1.00
Peak base width (°2Theta):	2.00
Minimum significance:	0.60

d-spacing (Å)	Relative Intensity (%)	Angle (°2Theta)	Peak Height (counts)	Background (counts)	Tip Width (°2Theta)	Significance
10.03882	2.34	8.80128	182.94	233.74	0.10027	1.26
9.20609	0.22	9.59917	17.00	214.77	0.10027	0.69
4.99832	2.15	17.73010	168.00	113.20	0.10027	1.00
4.26190	18.49	20.82531	1447.85	100.16	0.10027	4.24
3.85927	0.50	23.02624	38.77	92.75	0.20054	1.81
3.78316	0.26	23.49600	20.63	92.35	0.13369	0.77
3.69595	0.37	24.05862	29.27	91.87	0.33423	0.92
3.46743	0.52	25.67035	40.99	90.49	0.26738	0.63
3.35289	100.00	26.56308	7828.74	89.72	0.16711	28.42
3.22743	0.69	27.61568	53.64	88.82	0.33423	0.70
2.96621	0.94	30.10276	73.76	86.69	0.20054	2.13
2.46086	12.20	36.48172	955.07	72.64	0.13369	6.23
2.28357	6.05	39.42660	473.67	66.09	0.16711	6.98
2.24040	7.12	40.21872	557.37	65.69	0.13369	3.55
2.13108	4.23	42.37867	331.21	64.59	0.13369	2.21
1.99796	2.08	45.35380	162.54	65.82	0.10027	0.62
1.98194	9.16	45.74089	717.15	66.10	0.13369	5.44
1.85314	1.61	49.12206	125.70	59.93	0.10027	0.87
1.82007	11.84	50.07554	927.28	59.28	0.10027	2.58
1.81448	4.25	50.24033	332.77	59.17	0.06685	1.68
1.80372	1.11	50.56099	86.57	58.95	0.10027	2.09
1.67426	2.42	54.78352	189.79	58.65	0.13369	1.90
1.66117	1.54	55.25205	120.62	57.19	0.10027	0.96
1.54299	26.18	59.89572	2049.93	59.52	0.06685	1.76
1.53861	12.22	60.08403	956.67	59.16	0.06685	0.97
1.46932	0.12	63.23475	9.05	53.27	0.16711	0.69
1.45430	1.72	63.96479	134.35	53.58	0.10027	1.02
1.45014	0.68	64.16996	53.41	53.66	0.06685	1.20
1.41973	0.42	65.71511	33.24	54.31	0.06685	0.86
1.38311	7.88	67.68603	616.88	55.14	0.10027	2.32
1.37949	4.51	67.88748	352.88	55.23	0.06685	6.25
1.37592	6.99	68.08820	547.21	55.31	0.06685	0.66
1.37248	8.29	68.28192	649.32	55.39	0.06685	0.78
1.36900	2.66	68.47968	208.45	55.47	0.06685	4.61
1.34464	0.69	69.89893	53.80	56.07	0.10027	1.32
1.28889	6.73	73.40058	526.76	54.82	0.06685	0.74
1.28566	2.89	73.61566	226.57	54.72	0.10027	1.49
1.25658	3.72	75.61318	290.87	53.77	0.10027	1.69
1.25334	1.59	75.84315	124.76	53.66	0.10027	1.02
1.22926	3.38	77.60253	264.97	52.83	0.10027	2.23
1.22604	1.52	77.84478	119.15	52.72	0.10027	0.98

Philips Analytical

In this study, “The primary d-spacing peak matching method”was used to carry out the main silica building phases of the smoky quartzes. This method bases on a principle to match of the ideal primary d-spacing peak data for main silica building phases of ambient silica-bearing conditions according to the previously published the X-ray diffraction data with the primary d-spacing peak data provided from the investigated silica samples during this study.

In this method, the ideal X-ray diffraction data belonging to main silica building silica phases of the ambient silica bearing conditions (e.g. alpha-quartz, quartz-rich chalcedony, moganite, orthorhombic-silica, lutecite, opal-CT and opal-C) were compiled from the data given by American Mineralogist Crystal Structure Database; Elzea and Rice (1996); Florke et al. (1976, 1984 & 1991); Frondel (1985); Graetsch & Florke (1991); Graetsch et al. (1994); Guthrie et al. (1995); Heaney & Post (1992); Jones & Segnit (1971); Miehe et al. (1984); Miehe & Graetsch (1992); Murashov & Svishchev (1998); Smith (1992); ASTM cards 38-360; 38-448; 46-1045.

However, some peaks in the XRD graphics of this study were not able to match with the any given reference peaks.

Accordingly, dark brown colored smoky quartz samples were matched to the primary d-spacing peaks and relatively peak intensities of the 3.35 (100%)respectively. This valueis matched to the silica building phases signifying the Q-M. The fact states that natural smoky quartz samples are composed of mainly both alpha-quartz-Q (length-fast) and moganite-M (length-slow) silica building phases. In addition, other length-slow silica building phases, such as lutecite-L and *o*-silica-*O*S also exist in the inner structure of those samples.

Several peaks in the XRD graphic of the dark brown colored smoky quartz sample are matched to mainly alpha-quartz-Q (12 times), moganite-M (12 times) and with partially *o*-silica-*O*S (2 times), and lutecite-L (2 times) silica building phases. The main diffraction peak (3.35 Å with 100% intensity) is also matched to both alpha-quartz and moganite (Q-M). Other peaks (fewer than 100% intensity) are matched to

alpha-quartz as 10 in 11, with moganite as 11 in 21, with *o*-silica as 2 in 17, and with lutecite as 2 in 3. No peak is matched to opal-CT and opal-C. The characteristic strong and distinctive diffraction bands centered at ~3.35 Å, ~1.54 Å, ~4.26 Å, ~2.46 Å, ~1.92 Å, ~1.82 Å, ~1.38 Å, and ~2.24 Å are present in the XRD graphic of the smoky quartz sample. The most distinctive peak is centered at ~3.35 Å that represents quartz and moganite combination (Q-M). The others mostly represent phase combinations, such as quartz, moganite and *o*-silica (Q-M-OS) and quartz, moganite and lutecite (Q-M-L) trio combinations, quartz and moganite (Q-M) dual combination. There are rarely any single components of quartz (Q and moganite (M)). Some unimportant diffraction peaks do not matched to any well-known silica building components.

It is seen that the numerical peak values obtained from XRD graphics give more certain results on the detection and separation of all the kind of silica building phases than the polarizing microscope images.

It is revealed that all the samples include all the kind of silica building phases (e.g. alpha-quartz, moganite, *o*-silica, lutecite, opal-CT and opal-C) according to the X-ray diffraction patterns even if they are different ratios. Moreover, the moganite phase is distinctively present in the silica mineral species as an interval phase during their formation mechanism.

3.3.3 Optical Absorption (OA)

The OA spectrum of the investigated sample indicates morion type smokycoloration is due to due to the no transmittance of light rays in the Vis region after absorbances of light rays at 375 nm in UV region, 450-490 nm and 600-640 nm in Vis region, and 730 nm in IR region (Figure 3.3). These aborbances also may be relation with the unusual oxidised small proportions of certain impurity ions by irradiation, such as Al(IV) from the total aluminium, Ti(V) from the total titanium, and Mn(III) from the total manganese respectively.In addition, the buoyancies of these absorbance peaks in the visible region produce the color hues between light

smoky and dark smoky colorations in the samples. Thus, the dark smoky coloration of morion becomes dull or pale in relatively longer times.

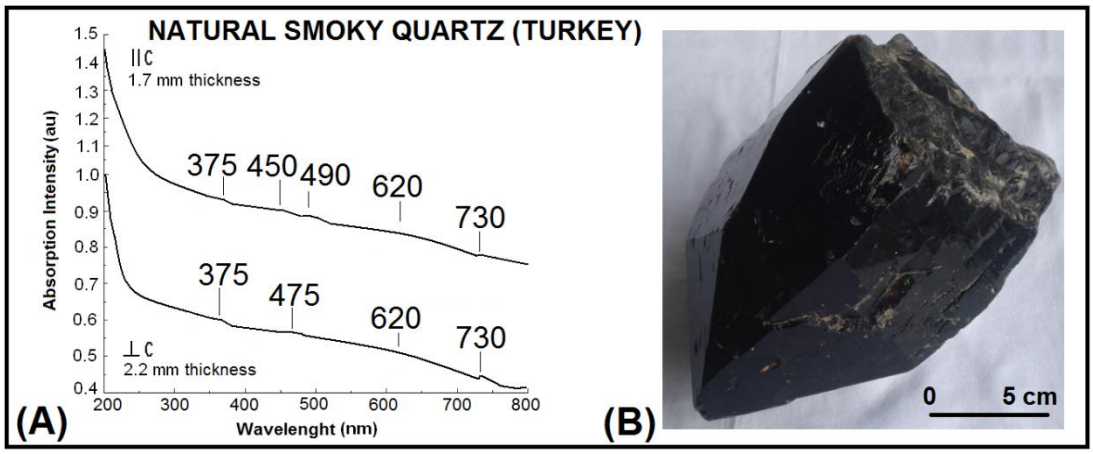

Figure 3.3 Optical absorption (OA) graphics (**A**), natural smoky quartz specimen of the Aydın region (**B**).

Optical absorption (OA) graphics (Figure 3.4) of initially dull or pale smoky quartz samples, after they were exposed to artificial gamma, neutron and beta irradiations depending on the various dose and periods, demonstrate that only gamma irradiation affect for color enhancement of the useless gem roughs. This situation demonstrates that the residue impurity elements except initial oxidised proportions of them are not mainly induced except a bit by any irradiation in a short period.

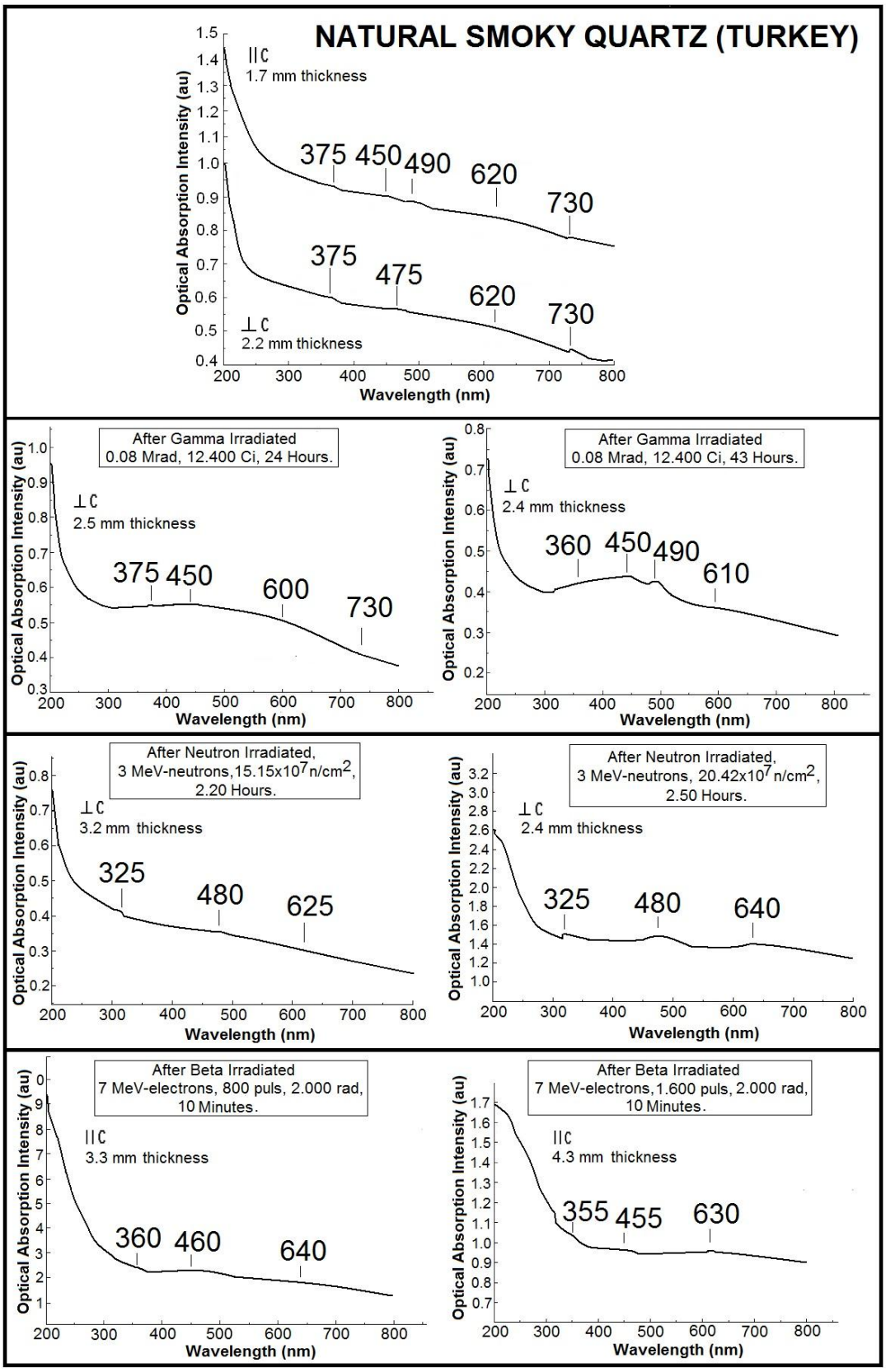

Figure 3.4 Optical absorption spectra (OA) of natural smoky quartz of Aydın region, and of after exposing to artificial gamma, neutron and beta irradiations (After Hatipoğlu et al., 2010).

3.3.4 Infrared Spectroscopy (IR)

Infrared stretching vibration spectra are widely used to reveal the presence of water in silica varieties. Absorption or transmission peaks in the infrared (IR) spectra of various single silicate minerals have been widely studied so far. Objectives of past studies have included the specific identification of mineral species, the detection, andcharacterization of the presence of water in these minerals (Ainworth, 2005; Aines & Rossman, 1984; Balitsky et al., 2004a and b; Brubach et al., 2005; Frondel, 1982; Fukuda & Nakashimi, 2008; Graetsch et al., 1985 & 1994; Harville & Britton, 1994; Heaney et al., 1994; Karampelas et al., 2005; Langer & Florke, 1974; Lind & Schmetzer, 1983; MSHA, 1994; Staats & Kopp, 1974; Stockton & Fritsch, 1987; Susuki, 1999; Taylor et al., 1970; Van Ginhoven et al., 2005; Yamagishi et al., 1997).

In this study, the IR transmission stretching curve of smoky quartz sampleswere recorded on standard axes in the measured range (4.000-400 cm^{-1}). They were compared with the some collective and crosswise vibration bands and peaks of the colorless quartz sample (Figure 3.5 and 3.6).

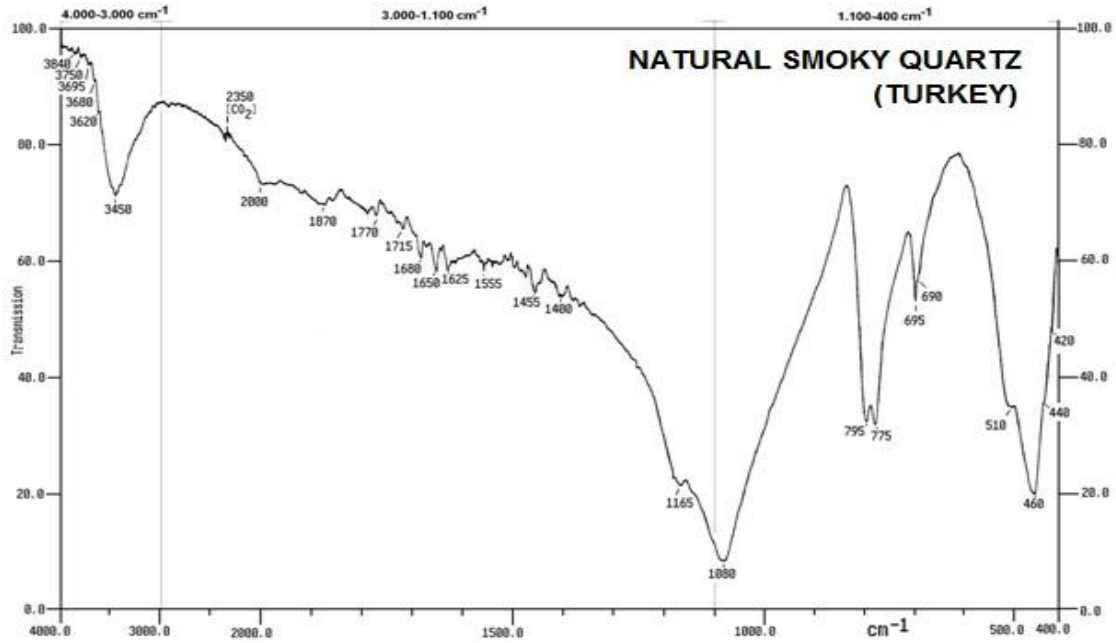

Figure 3.5 The IR transmission spectrum of natural morion type smoky quartz. The graphic was separated into three ranges—400-1.100 cm^{-1}, 1.100-3.000 cm^{-1}, and 3.000-4.000 cm^{-1}.

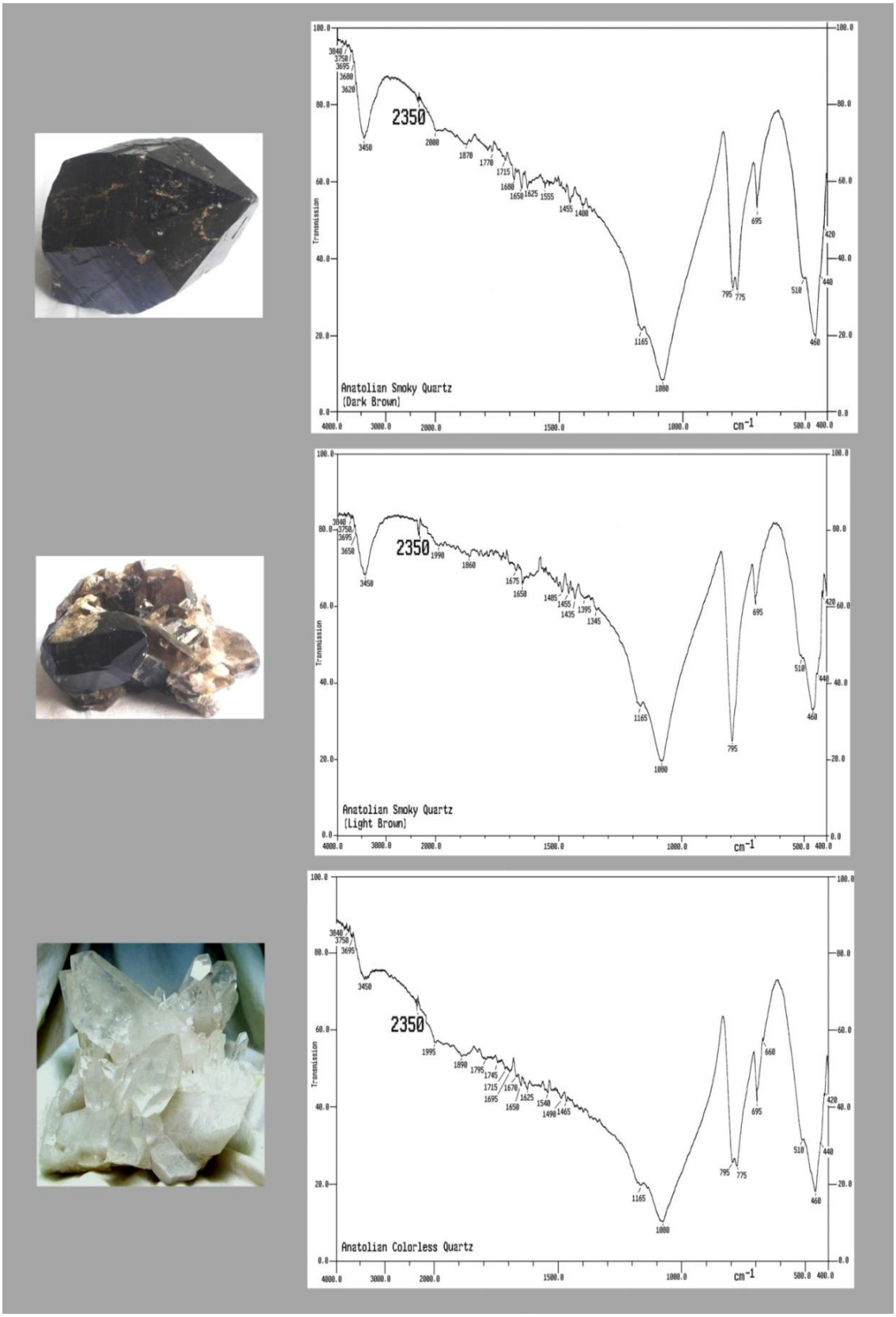

Figure 3.6 The IR transmission spectrum of natural dark (morion type), light smoky quartzes and colorless quartz for comparison and contrast to each other.

As seen the IR graphics, significant similarities and differences in the details of infrared vibrations in the certain ranges in the smoky quartzes are seen. For this reason, the infrared graphics of the investigated samples were separated into three ranges 400-1100 cm^{-1}, 1100-3.000 cm^{-1}, and 3000-4000 cm^{-1}.

The water vibrations have been reviewed with emphasis on natural single quartz varieties so far (Figure 3.7). It was reported by Dean (1999) there are generally three ranges for water in the absorption spectra of the minerals as follows;*700-930 cm^{-1},*1580-1750 cm^{-1}, and *2930-3650 cm^{-1}. On the other hand, the silanol water (SiOH) in the silica varieties are divided into three groups, namely SiOH group located at structural defects, surface silanols hydrogen bonded to each other and free surface silanols by Yamagishi et al. (1997). So, the water investigation on this study of natural silica mineral species from Turkey was discussed to base on the principles above mentioned.

The reversible reaction between molecular water and silica, e.g. Si-O-Si + H_2O = 2(Si-OH), is important for the diffusion of water in silica minerals (Van Ginhoven et al., 2005). In addition, the optical properties of silica varieties can be affected by the presence of water (Langer & Florke, 1974; Graetsch et al., 1985 & 1994; Heaney et al., 1994).In addition, Aines & Rossman (1984) reported that the distinction between very small inclusions and aggregates of structurally bound molecules is difficult, and that water molecules are the dominant hydrogen containing species in synthetic quartz but that this water is not in aggregates large enough to form ice when cooled.SiOH species in the infrared spectra decrease continuously even after the dehydration of most of H_2O molecules (Yamagishi et al., 1997). In investigations of IR absorption or transmission spectra, both specific characteristic peaks of the bands and those of molecular water (H_2O) and silanol groups ($Si\text{-}OH^-$) must be considered along with the peaks in the bands for all kinds of silica minerals (Taylor et al., 1970; Langer & Florke, 1974; Staats & Kopp, 1974; Lind & Schmetzer, 1983; Stockton & Fritsch, 1987; Smith, 1992; Graetsch et al., 1994; Balitsky et al.,2004a,b; Karampelas et al., 2005).

The first vibration range, 400-1100 cm^{-1}

The vibration range between 400 and 1100 cm^{-1} includes the most important transmission peaks to identify the silica building phases as well the water (700-930 cm^{-1}, Dean, 1999). For the comparison, ideal infrared (IR) graphic in the range of 600 cm^{-1} and 900 cm^{-1} for Quartz (Q), Cristobalite (C) and Amorphous Silica (AS) was shown in Figure 3.7 as complied by Ainsworth, 2005; MSHA, 1994). It is seen that quartz, cristobalite and amorphous silica have collectively transmission peaks to be characteristic for the silica varieties at near 800 cm^{-1} of IR graphic. In this study, the characteristic peak arises at 795 cm^{-1} of IR graphics of the investigated smoky quartz samples (Table 3.3).

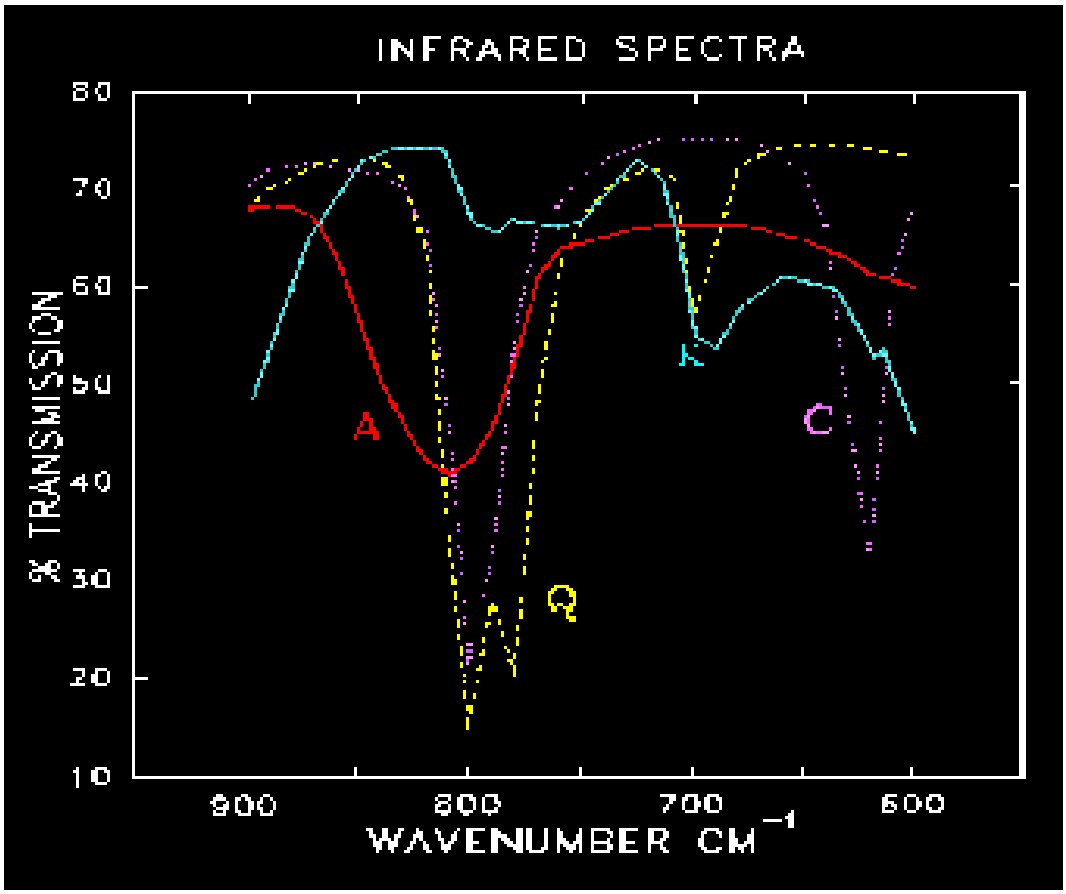

Figure 3.7 Ideal infrared (IR) graphic in the range of 600 cm^{-1} and 900 cm^{-1} for Quartz (Q), Cristobalite (C) and Amorphous Silica (AS) (from Ainsworth, 2005 & MSHA, 1994). Quartz, cristobalite and amorphous silica have a transmission peak at near 800 cm^{-1}.

In this part of the transmission spectrum, four significant and very strong transmission bands were collectively found in the investigated smoky quartz samples: first band centered at 460 cm^{-1}; second band centered at 695 cm^{-1}; third band centered at 795 cm^{-1}; and the fourth band centered at 1080 cm-1. In addition, there are a lot of peaks jointed to these main bands as shoulders. The IR bands are as follows;

The first band centered at 460 cm^{-1}

The first transmission band centered at 460 cm^{-1} includes three shoulders centered at 420, 440, and 510 cm^{-1} for both smoky quartz. The band was offered for halogen compounds by Dean (1999). According to this assumption, the first band centered at 460 cm^{-1} may be attributed to Si bonded halogen impurities in the investigated silica varieties (e.g. Br, I, Cl etc). On the other hand, the main band and its shoulders are corresponding with the data of Heaney et al. (1994). The authors reported some peaks centered at 410, 420, 430, 440, 451, and 460 cm^{-1} on this band in their study on the infrared spectrometry of silica.

The second band centered at 695 cm^{-1}

The spectra of the investigated smoky quartz samples show the transmission peak centered at 695 cm^{-1}. Heaney et al. (1994) reported that when this peak did not present in the spectrum of a silica variety, that sample did not include the alpha-quartz that represents characteristic of a crystalline structure. The second transmission band centered at 695 cm^{-1} includes one shoulder centered at 690 cm^{-1} for smoky quartz.

The third band centered at 795 cm^{-1}

A transmission band is centered at 795 cm^{-1}. In addition, a shoulder transmission peak at 775 cm^{-1} is also clearly present in the spectra. Smith (1992) has reported that cristobalite, tridymite, kaolinite, and amorphous silica have absorption peaks at near

800 cm^{-1}. Furthermore, MSHA (1994) is also informed that quartz, cristobalite and amorphous silica have collectively transmission peaks at near 800 cm^{-1}(Figure 3.6). In this study, this peak becomes clear centered at 795 cm^{-1}. On the other hand, Dean (1999) stated both that the range 700-930 cm^{-1} also belongs to water including of silica minerals, and that the range 860-760 cm^{-1} has Si-C accompanied by CH_2 rocking. It is possible that the water in this region will be attributed to surface silanols hydrogen bonded to each other from the SiOH species divided into three groups in natural silica varieties (Yamagishi et al., 1997; Graetsch et al., 1985 & 1994). According to this, a shoulder transmission peak centered at 775 cm^{-1} to be present in the spectra.

The fourth band centered at 1080 cm^{-1}

As being similarity, the absorption peak at 1080 cm^{-1} is uniformly present in the spectra of the investigated samples. The range 1000-1080 cm^{-1} is offered for (≡Si-O-Si≡) structure (Dean, 1999).As a result of these IR peaks, it can be stated that crystalline shaped silica varieties occur embedded in moderate silica-bearing ambient conditions because of their IR peaks belonging to the silica building phases.

Table 3.3 The infrared (IR) vibration peaks in the ranging between 400 and 1100 cm^{-1} of natural morion type smoky quartz sample.

Vibration Ranges	Ideal Vibration Peaks		Vibration Peaks in This Study
400-1100 cm^{-1}			
			420
			440
		460	**460**
			510
	Cristobalite	**620**	
			690
	Quartz	**695**	**695**
		775	**775**
	Quartz Cristobalite	**795**	**795**
	Amorphous Silica	**810**	
	Quartz	**1080**	**1080**

The second vibration range, 1100-3000 cm^{-1}

In this region, the infrared stretching vibrations of the investigated smoky samples have a complex curve.

The two transmission peaks centered at 1165 and 2000 cm^{-1} in each two sides of the second vibration range are remarkable (Table 3.6). These are also uniformly and very clear present in the spectra of the smoky quartz samples. So, it can be considered a characteristic transmission peak, whereas the characteristic presences of these peaks in all kinds of natural silica varieties have not been reported before. However, as being similarity, these peaks may be also related with Al ions bonded to SiO_4 tetrahedersas structural point defects (AlO_4).

One from the three ranges for water in the infrared spectra of the minerals is the region at 1580-1750 cm^{-1} (Dean, 1999). So, the spreading out and complexity of the peaks in the transmission spectra at about 1640 cm^{-1} and between 1620 cm^{-1} and 1660 cm^{-1} can be attributed to the vibration of water species, both molecular (H_2O) and silanol groups (SiOH) (Dean, 1999; Graetsch et al., 1994; Langer & Florke, 1974; Smith, 1992; Taylor et al., 1970).

There is a clear vibration thick about at 2350 cm^{-1} in the spectrum. This is due to CO_2 in the instrument if the carbon dioxide content of the instrument changes between the time the sample and the background are run. In addition, there most likely is also water vapor if there is carbon dioxide in the instrument.

The peaks at about 1545 and 1715 cm^{-1} become clear only macrocrystalline smoky quartz, so it may be related with water of crystallisation in high temperature crystals (Dean, 1999).

Table 3.4 The infrared (IR) vibration peaks in the ranging between 1100 and 3000 cm^{-1} of natural morion type smoky quartz sample.

Vibration Ranges	Ideal Vibration Peaks		Vibration Peaks in This Study
1100-3000 cm^{-1}	Al bonded to SiO_4 tetraheders	**1165**	1165
	Iron ion	**1240**	
	Iron ion	**1335**	
	Iron ion	**1360**	
			1400
			1455
	Water of Crystallisation	**1545**	1555
	Water	**1625**	1625
	Water	**1640**	1650
			1680
	Water of Crystallation	**1715**	1715
			1770
			1870
	Al bonded to SiO_4 tetraheders	**2000**	2000
	CO_2	**2350**	2350

The third vibration range, 3000-4000 cm^{-1}

This region in the spectrum has been the most studied region so far. In general, in the IR spectra of various silica varieties, the asymmetric strong transmission peak at about 3400 cm^{-1} between 3000 cm^{-1} and 3750 cm^{-1} is attributed to the vibration of both molecular (H_2O) water and silanol-groups water ($SiOH^-$) (Dean, 1999; Graetsch et al., 1985 & 1994; Langer & Florke, 1974; Smith, 1992; Taylor et al., 1970).

A number of peaks in the IR spectrum have been identified as indicating the specific presence of quartz. The 3595 cm^{-1} peak (Karampelas et al., 2005); the 3542 cm^{-1}, 3630 cm^{-1}, 3664 cm^{-1}, and 3684 cm^{-1} peaks (Balitsky et al.,2004a;2004b); and the structure of the 3000-3400 cm^{-1} band of the spectrum (Balitsky et al., 2004b) have all been reported as diagnostic and useful for distinguishing natural quartz from synthetic one. In addition, the band of the spectrum around 3400 cm^{-1} has shown to be useful for the separation of natural from synthetic alpha-quartz.

In this study, as being similarity, one significant and very strong transmission band was appeared at 3450 cm^{-1}(Table 3.5). This band with V-shaped is asymmetric characteristically, and due to the vibration of both molecular (H_2O) water and silanol-groups water ($SiOH^-$). In many situations, water in trace amounts KBr discs shows a broad band centered at 3450 cm^{-1} (Dean, 1999).

The investigated smoky quartz samples show some additional peaks as shoulders on this main band. As being similarity, the peak appeared at 3750 cm^{-1} is individual. So, this peak may be related to naturalness for the investigated sample. Other shoulders were not able to relate to any individuals.

Table 3.5 The infrared (IR) vibration peaks in the ranging between 3000 and 4000 cm^{-1} of natural morion type smoky quartz sample.

Vibration Ranges	Ideal Vibration Peaks		Vibration Peaks in This Study
3000-4000 cm^{-1}	Water	**3450**	3450
			3620
			3680
			3695
	Naturalness	**3750**	3750
			3840

3.3.5 Simultaneous Differential Thermal and Thermo Gravimetric Analysis (DTA/TGA)

General thermal behaviors of macrocrystalline silica mineral species were discussed before. However, these studies generally were on the single silica mineral specie (Brown et al., 2007; Checchetto et al., 1999; Esenli et al., 2001; Herdianita et al., 2000).

Thermal behaviors of the natural macrocrystalline smoky quartz samples were investigated using the thermograms of the simultaneous differential thermal and thermogravimetric analyses (DTA/TGA) from room temperature up to 1400 ^oC to observe the changing ratios in their water contents and enthalpy during dehydration. The related thermograms were given in Figure 3.8 and Tables 3.6 and 3.7

Relationships between the dehydration and sintering mechanisms of the investigated samples were shown on DTA/TGA glove curves. As a result of gloving up to 1400 ^{o}C, the gem quality transparent smoky quartz samples were sintered, and also their appearances were became opaque-white.

Smoky quartz samples have been heated from 27.75 ^{o}C to 1400 ^{o}C. When considered mass change of smoky quartz (TGA), material of 57.51 mg at the beginning has increased 58.66 mg after experiment. Accordingly, total mass change of solid smoky quartz observed in its thermogram is +1.15 mg in the process of being heated from room temperature (24.75 °C) to 1400 °C. Its rational value is, however, +1.200%. Also, a linear mass increase has been observed in TGA thermogram of macrocrystalline smoky quartz sample.

When considered enthalpy change of smoky quartz (DTA); it can be said that there were both an enthalpy decrease (endothermic) and an enthalpy increase (exothermic) from the beginning of heating to 1400 °C. However, the most typical event in DTA thermogram is an extraordinary exothermic and endothermic enthalpy change ranging from 579.95 °C and 584.90 °C. This curve's peak value is 575.95 °C. As a result, there are six physical processes in temperature (24.75-1400 °C) and energy range (0.0, -50.0 μV) in DTA thermogram of smoky quartz sample.

As taken into consideration all thermal behaviours of the smoky quartz samples, it can be stated that the macrocrystalline smoky quartz samples found occur embedded in the moderate silica-bearing ambient conditions of the hydrothermal solutions because their water implications and ratio between water (molecular) and water (SiOH) are almost high.

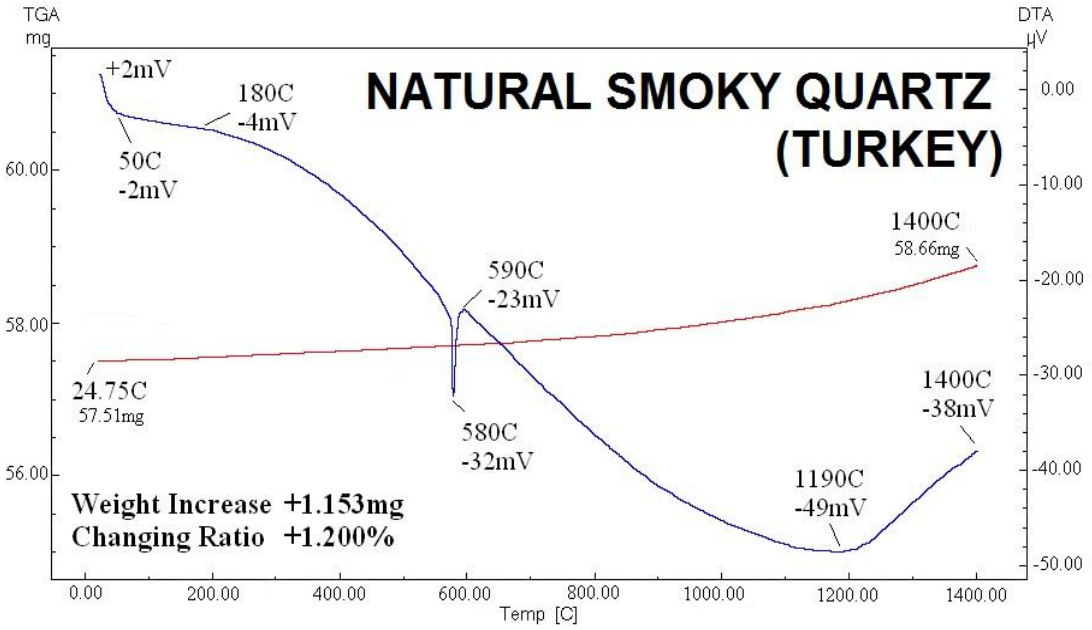

Figure 3.8 Simultaneous DTA/TGA thermogram of natural morion type smoky quartz. The red line on the thermogram represents the thermogravimetric glow curve, although the blue line represents the differential thermal glow curve.

Table 3.6Thermogram data of weight change (TGA) of natural morion type smoky quartz.

(Ratio of total weight change = +1.200%).
Range in which weight increases (24.75 – 1400 °C) ↑ 57.51 mg – 58.66 mg = +1.15 mg (+1.200%)

Table 3.7 Thermogram data of endothermic and exothermic cumulative temperature change (DTA) depending upon differentiation of smoky quartz.

Range in which enthalpy decreases (24.75 ^{o}C - ~50 ^{o}C) and (~+2.0, ~-2.0 µV = -4.0 µV)
Range in which enthalpy decreases at minimum level (~50 - ~180 ^{o}C) and (~-2.0 - ~-4.0 µV = -2 µV)
Range in which enthalpy decreases at maximum level (~180 - ~580 ^{o}C) and (~-4.0 - ~-32.0 µV = -28 µV)
Range in which enthalpy increases at minimum level (~580 - ~590 ^{o}C) and (~-32.0 - ~-23.0 µV = +9 µV)
Range in which enthalpy decreases at maximum level (~590 – 1190 ^{o}C) and (~-23.0 - ~-49.0 µV = -26 µV)
Range in which enthalpy increases at maximum level (~1190 – 1400 ^{o}C) and (~-49.0 - ~-38.0 µV = +11 µV)

3.3.6 Thermoluminesence Spectroscopy (TL)

External physical effects such as ionizing radiation, mineralization processes and temperature conditions cause defects within minerals. These defects are capable of trapping electrons and holes (sites which have lost an electron). These electrons and holes are produced by ionising radiation, either in nature (measured as the natural TL) or in the laboratory (measured as artificial TL). Most electrons and holes recombine almost immediately but in non-conducting minerals, a small percentage of the holes and excess electrons may be trapped on lattice defects and impurities(Townsend, 1994).

Smoky quartzes were often used in TL investigations of mineral deposits, a well known hole trap is a silicon site in which Al^{3+} has been substituted for Si^{4+}. Electrons can also be trapped, and this usually occurs on vacant oxygen sites where O^{2-} charge is missing. Initially the number of hole traps in quartz may be expected to be larger than the number of electron traps, but as the number of holes and electrons eventually trapped must be equal, the electron trapping mechanism becomes the predominant factor affecting the resultant strength of the TL signal.These trapped charges can be released by thermal activation which facilitates recombination of the holes and electrons. If recombination occurs at a specific site it may result in the emission of a quantum of visible light. This light can be measured and recorded as a glow peak. As electrons and holes may be trapped on a variety of sites with different crystal field energy, different amounts of thermal activation will be required to release them, and so over a range of temperatures a number of glow peaks are recorded which constitute a glow curve. Quartz typically gives several major glow peaks, and in particular, those at approximately 190°C, 260°C, and 350°C, with subordinate peaks at 150°C and 220°C. A major peak at 110°C may also appear. In this study, Figure 3.9 shows that the two peak values at 220°C as the perpendicular to "C" axisand at 210°C as the parallel to "C" axis in the thermoluminescence (TL)spectra is characteristic for morion type smokyquartz samples from the Aydın region. This peak valuescan be attributed to some extraordinary aluminium and iron element contents.In addition, the intensity and shape of the glow curves in the

samples depend on a number of factors such as lattice vacancies and mainly aluminium and iron capable of acting as traps, respective crystal field energies, and trap densities and charged occupancies. Several of these factors including the charge occupancy rate are a function of, and are affected by, external physical effects where the term external physical effect refers to external influences such as ionizing radiation and mineralizing processes in the samples. Therefore, the charge occupancy affects the strength of the TL signal.

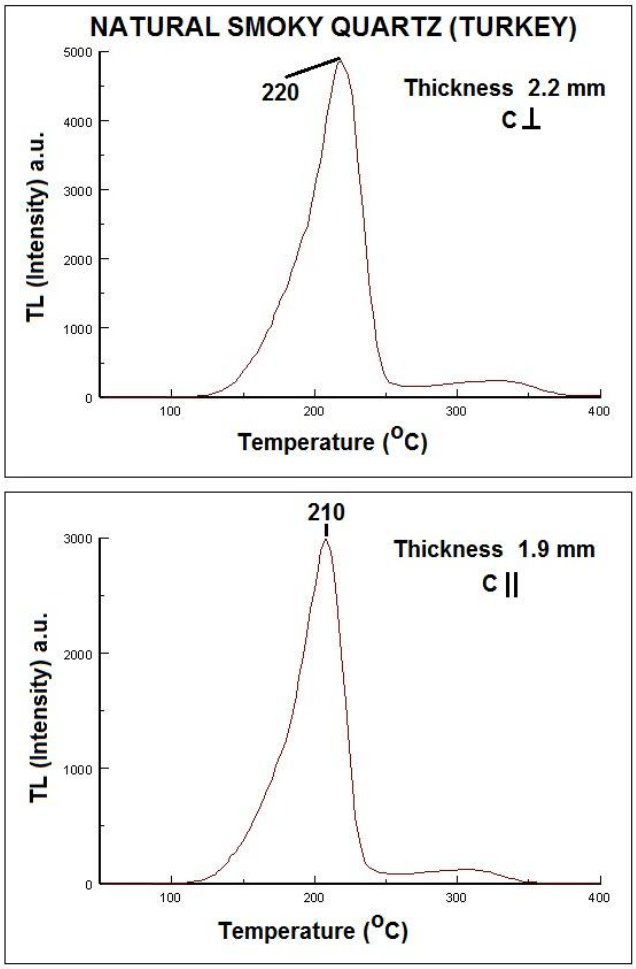

Figure 3.9 Thermoluminescence glow curves of natural morion type smoky quartz, taken from perpendicular to “C” axis and parallel to “C” axis.

3.3.7 Radioluminescence Spectroscopy (RL)

It is fact that the Fe(II) ion from the total iron, which is moreabundant in morion type smoky quartz crystals, based on the optical spectrum, is relativelyresistant to irradiation even if the ion is partially oxidized to Fe(III) ion by irradiation. Whilefinding these relationships, we first considered a comparison with the RL graphics (Figure 3.10)of both natural and synthetic quartz samples. We have concluded that the RL peak at 720 nmcertainly represents the oxidized Al(IV) ion. In conclusion, we can say that this RL study is moredistinctive than other luminescence data to detect the locations of the induced impurity elementswhen compared with previous studies (Hatipoğlu et al., 2010a).

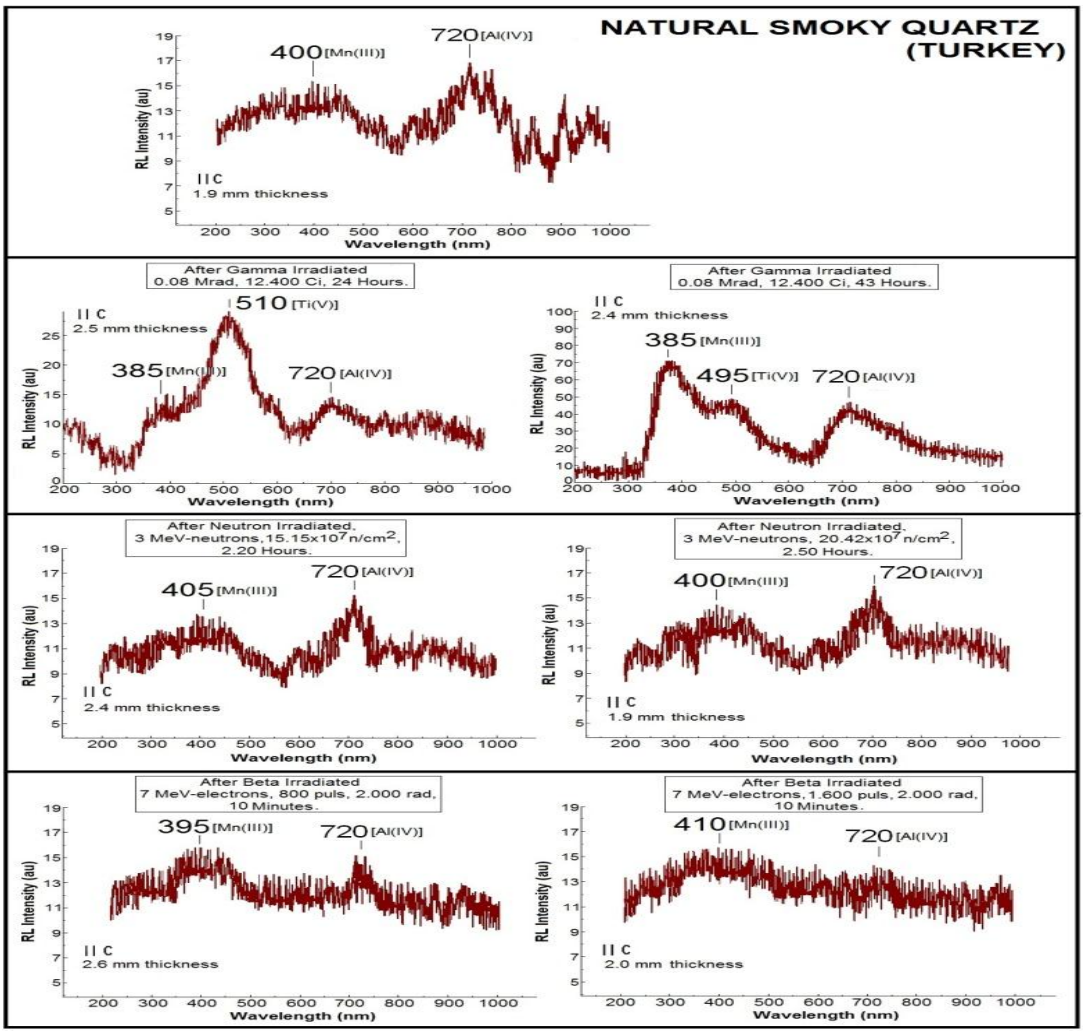

Figure 3.10 Radioluminescence (RL) spectra of natural and various irradiated smoky quartzes from the Aydın region (after Hatipoğlu et al., 2010a).

3.4 Gemmology

Smoky quartz can vary from grey to warm brown, light and clear to an almost "solid" looking black/brown. The coloration is due to natural radiation occurring in its environment.The crystals are quite hard, around seven on the Mohs scale, just under diamond which, along with concerns such as silicate dust makes these crystals challenging to cut. Most crystals are small in size with pyramidal ends. Often one end is broken off from a cluster leaving ragged edges and in order to use the crystals in jewelry those edges need to be cut. This can be done with good protection and the right tools. Several different methods can be used to cut through quartz crystal. They are collected into two basement methods; Facet cutting (Figure 3.11) and cabochon cutting (Figure 3.12). This includes using a wire saw, which can slice quartz into different pieces. CO_2 laser cutting is a process that is used to cut holes or shapes into quartz, which is effective on quartz countertops for drain cutouts and other holes needed. Water jet cutting, band saw slicing, and ID slicing are also different methods used for effectively cutting quartz crystal without damaging the material.



Figure 3.11 Facet cut and polished gemstones with various lapidary forms of light and morion type smoky quartz from the Aydın region. Two faceted smoky quartz stones mounted into a silver necklace (right).



Figure 3.12 Cabochon cut and polished gemstones with various lapidary forms of light and morion type smoky quartz from the Aydın region.

In today's gem market, Brazil is the largest producer and exporter of gem-quality smoky quartz crystals. However, Turkey is the other important producer and exporter of these crystals. Furthermore, none of these smoky quartz deposits has yet been mined professionally. When these deposits exploited, Turkey could be Brazil's competitor on the world market for smoky quartz.

The smoky quartz crystals in the Karacasu region are generally extracted as matrix specimens of various sizes. Crystals up to 180 kilograms have been collected, but most of the crystals vary between 0.3 and 5 kilograms.

In the Aydın-Koçarlı-Bağcılar and Esentepe regions (Figure 3.13), many promising veins and lenses of smoky quartz exist in an area of about eigth square kilometres. The deposit has been licensed to the private Mining Company. The distribution and structure of the quartz veins in the deposit has been investigated with field studies and seismic research. The smoky quartz veins generally have a width of 0.2 to 8 meters, a length of 1 to 7 meters, and a depth of 10 to 30 meters. The lenses

generally have a width of 0.5 to 2 meters, a length of 3 to 10 meters, and a depth of 3 to 6 meters. In summary, the Koçarlı Region's gem-quality smoky quartz deposit includes about 200.000 tons over a surface area of 8 square kilometres. If the lowest value is taken as 5,000 US dollars per ton, we estimate this area to have exploitable gem deposits worth about 1 billion US dollars.

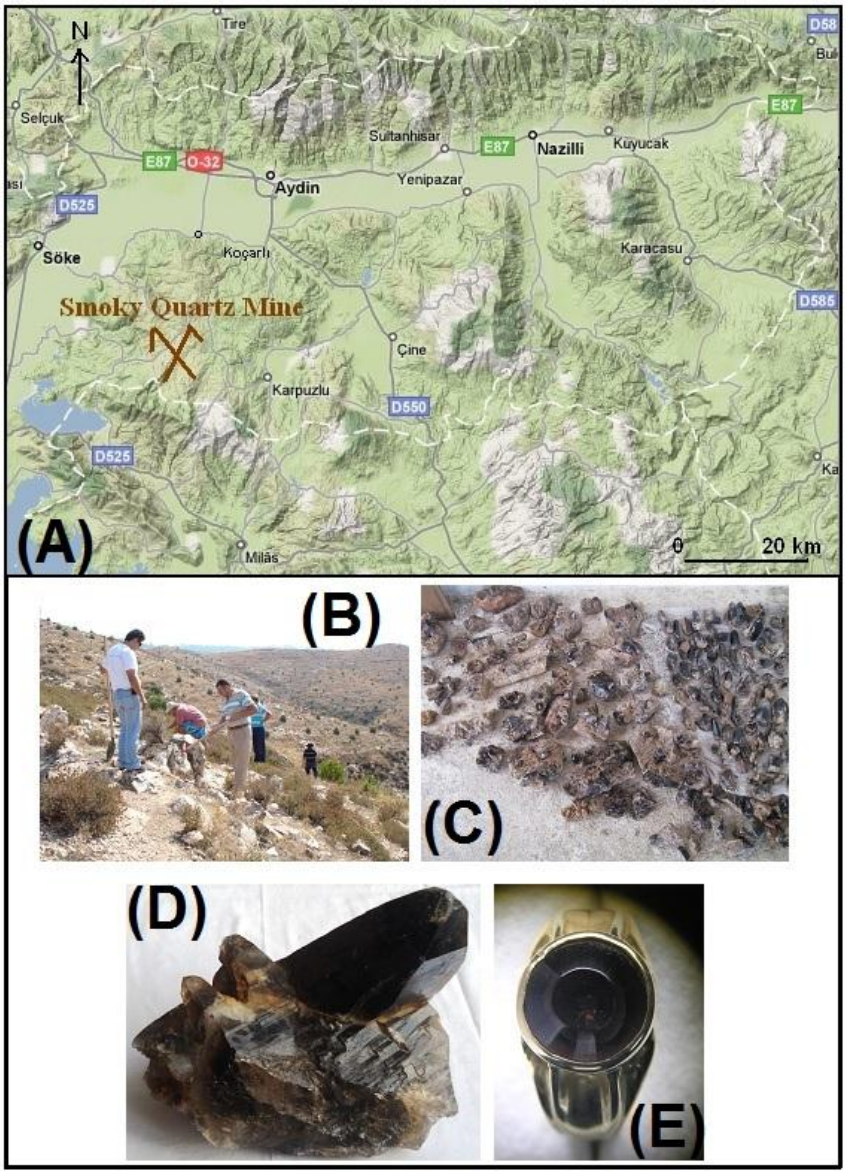

Figure 3.13 Smoky quartz mine field in the Aydın-Koçarlı-Bağcılar and Esentepe regions**(A)**. Quartz veins in gneiss and schist are exposed at the surface where they can be exploited by amateur gem hunters **(B)**. Stock of rough dark brown smoky quartz crystals (morion type **(C)**.Large crystal of them **(D)**. Faceted ring stone of this crystal, mounted on a gold ring **(E)**.

CHAPTER FOUR
CONCLUSIONS

In nature, colorless quartzes are routinely colored by irradiation with gamma rays. Similarity, synthetic colorless quartzes are also colored artificially by irradiation with gamma rays and heat-treatment for jewelry production now, because of more and more demand against to smoky quartz in the worldwide gem market.

The application of this material ina radiation environment often gives rise to deleteriouseffects: many investigations have suggested thatthese unwanted effects were associated with impuritiesand defects contained in the crystalline lattice,even when their concentration is in the ppm range. Al, Fe, Ti and Mn elements substituting for Si element in silica latticein the smoky quartz samples of Turkey are remarkable as ≥ 100 ppm. Colorless quartz becomes smoky or dark smoky (morion quartz) when exposed to gamma rays.Because the irradiation beams,in fact, affect all these impurity elements, these elements are responsible for the producing of the color centers for smoky coloration and luminescence peaks directly and indirectly.

The color saturation effect of irradiation on OA effects and RL signals from the aluminium, iron, titanium and manganese centresis tried to evaluatemorion typesmoky quartzesfrom the Aydın region.Accordingly, the OA spectra indicate dark smokycoloration in morion is due to no transmittance at visible region as a result of absorbance peaks at 375,450-490, 620 and 730 nm. These aborbances also may be relation with the unusual oxidised small proportions of certain impurity ions by irradiation, such as Al(IV) from the total aluminium, Ti(V) from the total titanium, and Mn(III) from the total manganese respectively.In addition, the buoyancies of these absorbance peaks in the visible region produce the color hues between light smoky and dark smoky colorations in morion samples. Thus, the dark smoky coloration of morion becomes dull or pale in relatively longer times. But, the RL spectroscopy of morion before and after they were exposed to gamma, neutron and beta irradiation beams demonstrates that the most induced ions from the irradiation are firstly Mn(III) and Al(IV), and secondly Ti(V). These ions represent the RL

peaks at about 400 nm, 720 nm and about 500 nm respectively. Ultimately,it is noted that Fe(II) ion from the total iron is relatively resistant against to irradiation even if the ion was oxidised to Fe(III) ion partially by irradiation.

As taken into consideration all thermal behaviours of the smoky quartz samples, it can be stated that the macrocrystalline smoky quartz samples found occur embedded in the moderate silica-bearing ambient conditions of the hydrothermal solutions because their water implications and ratio between water (molecular) and water (SiOH) are almost high.

Relationships between the dehydration and sintering mechanisms of the investigated samples were shown on DTA/TGA glove curves. As a result of gloving up to 1400 ^{o}C, the gem quality transparent smoky quartz samples were sintered, and also their appearances were became opaque-white.

The two peak values at 220°C as the perpendicular to “C” axisand at 210°C as the parallel to “C” axis in the thermoluminescence (TL)spectra is characteristic for morion type smoky. Quartz samples from the Aydın region. This peak valuescan be attributed to some extraordinary aluminium and iron element contents.

REFERENCES

Ainsworth, S.M. (2005). Infraredanalysis of respirable coal mine dust for quartz*:* Thirty-five years. *Journal of ASTM International, 2* (4), 1-13.

Aines, R.D., & Rossman, G.R.(1984). Water in Minerals?A peak in the infrared.*Journal of Geophysical Research, 89*(B6), 4059–4071.

Alfassi Z.B. (2000). In: Meyers RA, editor. *Encyclopaedia of analytical chemistry*.Chichester: John Wiley & Sons.

Back, M., & Mandarino, J. (2008). *Fleischer's glossary of mineral species* (10thEd.). Tucson: The Mineral Record Inc.

Bahadur, H. (1989). Infrared characterization of natural and cultured quartz: The effect of electro diffusion and irradiation.*Journal of Applied Physics, 66*, 4973-4982.

Bahadur, H.A. (1998). Brief survey of aluminium and alkali-related hydroxyl defects in quartz crystals and their radiation effects.*Radiation Physics and Chemistry, 51*, 513-514.

Brubach, J.B.,Mermet, A.,Filabozzi, A.,Gerschel, A., &Roy, P. (2005). Signatures of the hydrogen bonding in the infrared bands of water.*Journal of Chemical Physics, 18* (122), 184509 (7 pages).

Collins, A.S., & Robertson, A.H.F. (2003). Kinematic evidence for Late Mesozoic–Miocene emplacement of the Lycian Allochthon over the Western Anatolide Belt, SW Turkey.*Geological Journal, 38*, 295-310.

Dean, J.A. (1999). *Lange's handbook of chemistry* (15thed.). New York:Mc-Graw-Hill, Inc.

Flörke, O.W.,Florke, U. & Giese, U.(1984). Moganite-a new microcrystalline silica-mineral.*Neues Jahrbuch für Mineralogie Abhandlungen, 149*, 325-336.

Flörke, O. W.Graetsch, H.Martin, B.Roller, K. ,& Wirth, R., (1991) Nomenclature of micro- and non-crystalline silica minerals, based on structure and microstructure. *Neues Jahrbuch für Mineralogie Abhandlungen, 163*, 19-42.

Graetsch, H., Florke, O.W, & Miehe, G. (1987) Structural defects in microcrystalline silica. *Physics and Chemistry of Minerals, 14*, 249-257.

Halliburton, L.E., Koumvakalis, N.,Markes, M.E., & Martin, J.J. (1981). Radiation effects in crystalline SiO_2: The role of aluminium. *Journal of Applied Physics, 52*, 3565-3574.

Halliburton, L.E.(1989). ESR and optical characterization of point defects in quartz. *Applied Radiation Isotopes, 40*, 859-863.

Hatipoğlu, M.,Helvacı, C.,Kibar, R.,Çetin, A.,Tuncer,Y., & Can, N. (2010a). Amethyst and morion quartz gemstone raw materials from Turkey: color saturation and enhancement by gamma, neutron and beta irradiation.*Radiation Effects and Defects in Solids*, *165* (11), 876-888.

Hatipoğlu, M.,Babalık, H., & Chamberlain, S.C. (2010b). Gemstone deposits in Turkey. *Rocks & Minerals*, *85*(2), 124-132.

Hashimoto, T.,Yamaguchi, T.,Fujita, H., & Yanagawa, Y. (2003). Comparison of infrared spectrometric characteristics of Al-OH impurities and thermoluminescence patterns in natural quartz slices at temperatures below 0°C. *Radiation Measurement, 37*, 479-485.

Harville, D., & Britton, A. (1994). Identification and quantification of silica phases in the Monterey Formation using infrared spectroscopy. *AAPG Bulletin, 78*, 664-665.

Heaney, P.J.,Prewitt, C.T., & Gibbs, G.V., (Eds.). (1994). Silica, physical behavior, geochemistry, and materials aplications. *Reviews in Mineralogy,29*, Mineralogical Society of America, Washington, DC.

Heaney, P.J., & Banfield, J.A. (1995). Structure and chemistry of silica, metal oxides and phosphates. In Guthrie, G. D., and Mossman, B. T. (Eds.) Health effects of mineral dusts. *Reviews in Mineralogy, 28*, 185-233.

Iler, R.K. (1979). *The chemistry of Silica*.New York: J. Wiley & Sons.

Itoh, N.,Stoneham, D.,& Stoneham, A.M.(2002). Ionic and electronic processes in quartz: Mechanisms of thermoluminescence and optically stimulated luminescence. *Journal of Applied Physics, 92*, 5036-5044.

Kats, A. (1962). Hydrogen in α-quartz.*Philips Research Reports.,17*, 133-195.

Koumvakalis, N. (1980). Defects in crystalline SiO_2: Optical absorption of the aluminium-associated hole center. *Journal of Applied Physics, 51*, 5528-5531.

Krauskopf, K.B. (1982). *Introduction to Geochemistry* (2nd Ed.). Singapore: McGrowHill Book Co.

Lehmann, G., & Moore, W.J. (1966). Optical and paramagnetic properties of iron centers in quartz.*Journal of Chemical Physics, 44*, 1741-1745.

Lehmann, G. (1971). The structure of yellow color centers in quartz. *Physica Status. Solidi. 48*, K65-K67.

Loeffler, B.M., & Burns, R.G. (1976). Shedding light on the color of gems and minerals,*American Scientific, 64*, 636-639.

Miehe, G., & Graetsch, H. (1992). Crystal structure of moganite: A new structure type for silica.*European Journal of Mineralogy, 4*, 693-706.

Mine Safety and Health Administration. (1994). *Infrared determination of quartz in respirable coal mine dust:* Method P-7. Pittsburgh, PA: U.S. Department of Labor,.

Murashov, V.V., & Svishchev, I.M. (1998). Quartz family of silica polymorphs: Comparative simulation study of quartz, moganite, and orthorhombic silica, and their phase transformations.*Physical Review B, 57*, 5639-5646.

Nassau, K. (1978). The origins of color in minerals.*American Mineralogist, 63*, 219-229.

Nesse, W.D. (2004). *Introduction to optical mineralogy*. Oxford University Press.Inc. London.

Nunes, E.H.M., & Lameiras, F.S. (2005). The optical absorption of gamma irradiated and heat-treated natural quartz. *Materials Research, 8*, 305-308.

Pretola, J.P. (2001), A feasibility study using silica polymorph ratios for sourcing chert and chalcedony lithic materials. *Journal of Archaeological Science, 28*, 721-739.

Rodgers, K.A., & Cressey, G. (2001). The occurrence, detection and significance of moganite (SiO_2) among some silica sinters. *Mineralogical Magazine, 65*, 157-167.

Rossman, G.R. (1994). Colored varieties of the silica minerals.*Reviews in Mineralogy Geochemistry, 29*, 433-467.

Smith, D.K. (1992). The measurements of crystalline silica (Evaluation of the detectability and quantification of respirable crystalline silica by X-ray powder diffraction methods), *in: Proceeding of Crystalline Silica Panel 1-71.*

Staats, P.A., & Kopp, O.C. (1974). Studies on the origin of the 3400 cm^{-1} region infrared bands of synthetic and natural α-quartz. *Journal of Physics and Chemistry of Solid, 35*, 1029-1033.

Stockton, C.M., & Fritsch, E. (1987), Infrared spectroscopy in gem identification. *Gems and Gemology, 23*, 18-26.

Susuki, S. (1999).In-situ IR measurements of OH species in quartz at high temperatures. *Physics and Chemistry of Minerals, 26* (3), 217-225.

Townsend, P.D. (1994). Analysis of TL emission spectra. *Radiation Measurements 23*, 341–348.

Taylor, D.H.,Knoche, L., & Granwille, W.C. (1948). *Color harmony manual, descriptive color names dictionary.* Wilhelm Oswald System, Container Corporation of America, (2nd Ed.) Chicago.

Weil, J.A. (1984). Review of electron spin spectroscopy and its application to the study of paramagnetic defects in crystalline quartz. *Physics and Chemistry of Minerals, 10*, 149-165.

Van Ginhoven,R.M.,Jonsson, H.,Park, B., & Corrales, L.R. (2005). Cleavage and recovery of molecular water in silica. *Journal of Physical Chemistry B, 109*, 10936-10945.

Yamagishi, H.,Nakashima, S., & Ito, Y. (1997). High temperature infrared spectra of hydrous microcrystalline quartz. *Physics and Chemistry of Minerals, 24* (1), 66-74.